NASA TECHNICAL NOTE

NASA TN D-3632

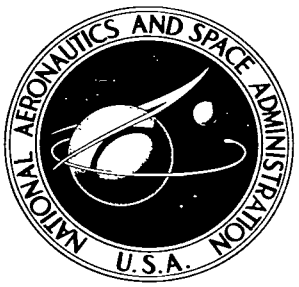

NASA TN D-3632

AN EXPERIMENTAL AND ANALYTICAL STUDY OF THE LONGITUDINAL VIBRATION OF A SIMPLIFIED THOR VEHICLE STRUCTURE

by Huey D. Carden and John P. Raney

Langley Research Center
Langley Station, Hampton, Va.

NATIONAL AERONAUTICS AND SPACE ADMINISTRATION • WASHINGTON, D. C. • OCTOBER 1966

NASA TN D-3632

AN EXPERIMENTAL AND ANALYTICAL STUDY OF THE LONGITUDINAL VIBRATION OF A SIMPLIFIED THOR VEHICLE STRUCTURE

By Huey D. Carden and John P. Raney

Langley Research Center
Langley Station, Hampton, Va.

NATIONAL AERONAUTICS AND SPACE ADMINISTRATION

For sale by the Clearinghouse for Federal Scientific and Technical Information
Springfield, Virginia 22151 – Price $2.00

CONTENTS

AN EXPERIMENTAL AND ANALYTICAL STUDY OF THE LONGITUDINAL VIBRATION OF A SIMPLIFIED THOR VEHICLE STRUCTURE

By Huey D. Carden and John P. Raney
Langley Research Center

SUMMARY

Results are presented of an experimental and analytical study of the longitudinal vibrational response of a simplified Thor vehicle. The empty, unpressurized vehicle was suspended horizontally with free-free boundaries and the longitudinal frequency response of the structure was obtained. Input and transfer impedance data between 5.0 cps and 200.0 cps indicated the existence of six major resonances with a large number of secondary responses between 55.0 cps and 168.0 cps. Two of the major resonances occurred at frequencies below the first structural longitudinal-mode frequency and were identified as the fundamental acoustic resonances of the empty liquid oxygen and fuel tanks. The ratio of structural damping to critical damping obtained by using the log decrement method, was also determined to be 0.025 and 0.033 for the first and fourth of the major structural modes, respectively.

Two analytical models were used to compute dynamic responses for comparison with the experimental data. Comparison of the experimental and analytical results indicate good agreement with both analytical models.

INTRODUCTION

Longitudinal vibrations which have occurred during the flights of large liquid propellant launch vehicles, including Thor-Agena, Titan, and Atlas (ref. 1), impose severe dynamic loads and vibration environments on unmanned spacecraft payloads. Such vibrations are of even greater significance for manned spacecraft since the tolerable vibration levels in the spacecraft are much lower. The condition commonly referred to as "Pogo" is an example of a longitudinal vibration response which has existed on current vehicles and potentially may exist on future launch vehicles. "Pogo" is a self-excited instability involving thrust oscillations, a longitudinal vibration mode of the vehicle, and variations in the propellant flow rate in the propellant lines and turbopumps. Flight data and analytical studies have indicated that a better understanding of the contribution, coupling, and interaction of the various structural components during longitudinal

vibrations is necessary to predict the structural dynamic aspects of a problem such as "Pogo." (See refs. 2 to 5.)

Very little experimental data have been obtained on the longitudinal vibration characteristics of typical launch vehicles. Therefore, in an attempt to understand better the longitudinal vibration properties of an actual launch vehicle structure and, specifically, a vehicle which has experienced the "Pogo" instability, the Langley Research Center is conducting an experimental and analytical investigation of the structural dynamic characteristics of a Thor-Agena launch vehicle. This paper presents the results of the first phase of this investigation which involved only the Thor stage of the launch vehicle structure. Longitudinal free-free vibration modes, frequencies, damping, and mechanical input and transfer impedances were measured on the empty, unpressurized vehicle in a horizontal position. An analytical investigation was also conducted in order to determine an equivalent system which would approximate the experimental results, to provide additional insight into the behavior of complex structures, and to indicate any weaknesses in analysis procedures. The experimental data are compared with analytical results from both a lumped mass-spring model and a continuous model derived by receptance techniques (ref. 6).

SYMBOLS

Measurements for this investigation were taken in the U.S. Customary System of Units. Equivalent values are indicated herein in the International System (SI) in the interest of promoting use of this system in future NASA reports.

A cross-sectional area, inch^2 (meter^2)

$a = \sqrt{E/\rho}$, inch/second (meter/second); also displacement location associated with free end of a spring

b displacement location associated with a mass element

$\frac{C}{C_C}$ damping ratio, $\frac{1}{2\pi n} \log_e \frac{Y_o}{Y_n}$

$\frac{c_p}{c_v}$ ratio of specific heat at constant pressure to specific heat at constant volume

E Young's modulus, pounds/inch^2 (newtons/meter^2)

F force, pounds (newtons)

$F_s(t)$ unit harmonic input force to structure, pounds (newtons)

f frequency, cycles/second

$j = \sqrt{-1}$

K stiffness or spring constant, pounds/inch (newtons/meter)

k any arbitrary point at which steady response is measured where k may be a, b, 0, 1, 2, . . . 7

L length, inch (meter); used with subscripts to indicate particular section of vehicle

l any arbitrary point of application of a force where l may be a, b, 0, 1, 2, . . . 7

M mass, $\frac{\text{pound-second}^2}{\text{inch}}$ (kilograms)

n number of cycles

p_o atmospheric pressure, pounds/square inch (newtons/meter^2)

t time, second

x coordinate along length of vehicle, inches (meters)

Y_n amplitude of nth cycle, inches (meters)

Y_o initial amplitude, inches (meters)

y,Y displacement and displacement amplitude, inches (meters)

α receptance (see eqs. (A17) to (A29)), inches/pound (meters/newton)

$\gamma = \frac{c_p}{c_v} = 1.4$

$\lambda = \frac{\omega}{a}$, radians/inch (radians/meter)

ρ	mass density, $\frac{\text{pound-second}^2}{\text{inch}^4}$ $\left(\frac{\text{kilogram}}{\text{meter}^3}\right)$
ω	angular frequency, $2\pi f$, radians/second

Subscripts:

1c	1st calculated
2c	2d calculated
1e	1st experimental
2e	2d experimental
E	denotes quantities associated with engine mass
F	denotes quantities associated with fuel and fuel tank bulkhead subsystem
FU	denotes quantities associated with fuel ullage
G	denotes quantities associated with guidance section
I1	denotes quantities associated with interstage area one (engine skirt)
I2	denotes quantities associated with interstage area two (center body)
kℓ	coordinates or locations at which response is measured and at which force is applied, respectively (k = a,b,0,1,2, . . . 7; ℓ = a,b,0,1,2, . . . 7)
L	denotes quantities associated with LOX and LOX tank bulkhead
LU	denotes quantities associated with LOX ullage
MWF	denotes quantities associated with mass M_{WF}
MI1	denotes quantities associated with mass M_{I1}
MI2	denotes quantities associated with mass M_{I2}
MWL	denotes quantities associated with mass M_{WL}

p denotes quantities associated with payload mass

TF denotes thrust frame

TP denotes turbopump

WF denotes quantities associated with walls of fuel-tank section

WL denotes quantities associated with walls of LOX tank section

Superscripts:

LU denotes path into LOX ullage of superscripted quantities

WL denotes path into walls of LOX tank of superscripted quantities

WF denotes path into walls of fuel tank of superscripted quantities

F denotes path into fuel and fuel tank bulkhead of superscripted quantities

Matrix notations:

{ } column

[ ] square

Dots over symbols indicate derivatives with respect to time.

APPARATUS AND EXPERIMENTAL PROCEDURE

Description of Vehicle

An empty, unpressurized, structurally complete Thor vehicle was suspended horizontally. Photographs and sketches of the vehicle, instrumentation locations, and testing apparatus are given in figures 1 to 7 and in tables I and II. Measured weights and center-of-gravity locations of the vehicle and of the various structural components are given in table I. Instrumentation locations are presented in table II.

General description.- The Thor vehicle airframe (figs. 1 and 2) is of semimonocoque construction and is nominally 56.7 feet (17.3 m) long. The assembly consists of five basic sections: the guidance section, fuel tank section, center-body section, liquid

oxygen (LOX) tank section, and engine and accessories section. The mass and stiffness distribution for the vehicle is given in figure 8. The vehicle is 8 feet (2.44 m) in diameter throughout the nontapered sections; however, forward of the center body, the airframe tapers from an 8-foot (2.44 m) diameter at the aft end of the fuel tank to a 6-foot (1.83 m) diameter at the forward end of the guidance section. The vehicle was simplified in that certain nonstructural components, including the engines, were removed. The mass of the empty simplified vehicle was 5029 lbm (2281 kg) compared with a nominal 6431 lbm (2917 kg) for a typical Thor.

Guidance section.- Figure 3 shows an interior view of the guidance section which is approximately 9 feet (2.74 m) long and tapers from 5.4 feet (1.65 m) in diameter across the forward end at Thor station 42.06 to 6.25 feet (1.90 m) in diameter at station 151.00 where it attaches to the fuel-tank section. Two equipment racks in the section provide platforms for mounting guidance and electrical equipment normally included in the guidance section. For the tests reported herein, all equipment and wiring were removed. Added strength and rigidity are provided by stringers and ring frames attached to the aluminum skin. The section is bolted to the fuel-tank section through an attach angle at station 151.00.

Fuel-tank section.- The fuel-tank section (fig. 4) is approximately 15.5 feet (4.72 m) long and tapers from 6.25 feet (1.90 m) in diameter across the forward end at Thor missile station 151.00 to 8 feet (2.44 m) in diameter at the aft end at station 336.00. The inner surface of the aluminum tank skin is machined in a 45° waffle pattern. Added strength and rigidity is provided by three frames attached to the skin. Attach angles at the forward and aft ends provide means for bolting to the adjacent section.

Center-body section.- The center-body section (fig. 5) structurally joins the fuel and liquid oxygen tank sections. The section is approximately 33 inches (0.838 m) long and is 8 feet (2.44 m) in diameter extending from station 336.00 to station 369.00. The section is constructed of aluminum skin and aluminum stringers. Aluminum angles are riveted to the forward and aft ends of the skin to provide for attachment to adjacent sections. The section has two hinged access doors and two nonhinged access panels. Cutouts for entrance of tubing and wiring are also provided.

Liquid-oxygen (LOX) tank section.- The liquid-oxygen tank section (figs. 5 and 6) is approximately 22.33 feet (6.80 m) long with a constant 8-foot (2.44 m) diameter from the forward attach angle at station 369.00 to the aft end at 636.67. The construction is similar to the fuel tank with the 45° internal waffle pattern. The aft portion of the LOX tank section, station 602.50 to 636.67, is referred to as the skirt section (fig. 6). The section consists of aluminum skin riveted to frames and aluminum stringers. A fuel-transfer tunnel (fig. 1(a)) extends through the LOX tanks. The aluminum-alloy tube has

expansion joints at either end. Attach angles are provided for bolting of the LOX tank to adjacent sections.

Engine and accessories section.- The engine and accessories section (fig. 7) is approximately 7 feet (2.13 m) long and is 8 feet (2.44 m) in diameter from the forward attach angle at station 636.67 to station 722.00. The section consists of aluminum skin riveted to aluminum stringers and aluminum frames. The forward and aft ends of the skin are attached to built-up frames of aluminum angles. Three thrust beams 120° apart extend the length of the section. The thrust fittings at station 636.67 provide the attach points for the engine mount. Three launch beams located midway between the thrust beams extend from 688.00 aft to station 722.00. The launch beams are built-up beams of forged and machined fittings, aluminum angles, and webs. The main engine thrust chamber, engine gimbal, vernier engine shields, engine hydraulic actuators, and other miscellaneous items were removed from this section.

Instrumentation

The vehicle was instrumented with linear servo accelerometers (table II) placed with their sensitivity axes parallel to the longitudinal axis of the vehicle at the base of the engine thrust frame (station 677.80), bottom and top of the LOX tank (stations 602.50 and 369.00, respectively), bottom and top of the fuel tank (stations 336.00 and 151.00, respectively), and at the top of the guidance section (station 42.06). The frequency response was flat from zero to approximately 250 cps. The accelerometers were 120° apart on the structure in bays A and B (see table II) and on a line running the length of the vehicle through two of the thrust-frame-attachment points. The input force and acceleration at the apex of the thrust frame, the shaker attachment point, were also recorded. The acceleration signals were recorded on an oscillograph while the force level was read from a calibrated peak reading meter and monitored on an oscilloscope. Excitation was provided by a 3000-pound-force (13,344 N) hydraulic shaker (fig. 2). Frequencies were obtained from an electronic frequency counter.

Experimental Procedure

The Thor vehicle was suspended horizontally on nylon straps located at stations 151.00 and 636.67 from overhead A-frames (fig. 2). Sinusoidal longitudinal response data were obtained at desired force levels and frequencies. Data were obtained in this manner through a frequency range (5.0 cps to 200.0 cps) which included the four major longitudinal modes of the structure. The input force and resulting input accelerations at the gimbal point were obtained for the following conditions: (1) both the fuel and the LOX tank closed and containing unpressurized air, (2) both ends of the fuel tank and the top of LOX tank vented, and (3) both ends of the fuel tank vented and the LOX tank containing an

unpressurized mixture by volume of 50-percent helium and 50-percent air. Response data along the length of the vehicle were also obtained for condition 3. In addition to the tests on the structurally complete vehicle, tests were also made to determine the first free-free longitudinal mode of the vehicle with the guidance section removed. The purpose of obtaining data for this vehicle configuration was to provide quantitative information on the effect of removing a major section of the structure.

For the purpose of determining the structural damping by the log decrement method for two longitudinal modes, a vacuum coupling was used between the vibration exciter and the Thor vehicle which permitted quick disconnecting of the exciter from the structure.

The individual natural frequencies of the turbopump and of the engine thrust structure were determined by exciting these components separately and observing the period of free oscillation.

ANALYSIS

Analytical Model Representations

Analytical models were constructed for calculating the longitudinal modes and, in some instances, the forced response levels for sinusoidal input to the vehicle. Two basic concepts were employed, both of which assumed that the vehicle behaved essentially as a one-dimensional bar in the longitudinal direction. The first model treated the structure as a series of spring connected lumped masses and is a standard approach as discussed in reference 7. The second model allowed the vehicle, together with the contained ullage gas to be treated as a continuous system. The method of solution to the equations of motion for each of the analytical models is discussed in the section "Method of Solution" and in the appendix.

Lumped-mass model.- The lumped-mass model was an 8-mass representation (illustrated in table III). The mass lumping procedure used was to concentrate masses equal to one-half the mass of each basic section of the vehicle (see fig. 8(a)) and to connect these masses by an elastic spring K, determined from the stiffness distribution (see fig. 8(b)) of that section by using the formula $K = \frac{AE}{L}$. The representation of the complete vehicle was then achieved by superposition. Branches were allowed for the engine thrust structure and the turbopumps for which the uncoupled frequencies, determined experimentally, were in the frequency range of interest. The spring constants for these branches, shown in table III, were calculated from the known masses and uncoupled frequencies. In addition, the model for the structurally complete Thor vehicle, a 7-mass representation (given in table IV) was used for computing the modes of the vehicle without the guidance section.

Continuous model.- In contrast to the one-dimensional, lumped-mass model which approximates continuous structures as discrete masses and springs, the mathematical model designated as the continuous model and shown in figure 9 allows the structure and the ullage gas in the tank sections to be treated as one-dimensional continuous systems. The structural elements are replaced with uniform bars having a cross-sectional area, density, and length equivalent to the shells which they replace. Any masses unaccounted for by the bars are lumped at the ends in such manner as to make the continuous model consistent with the lumped-mass model. Thus, the continuous model may be derived from the lumped-mass model and vice versa, and both models are consistent with the data given in tables I and II and figure 8. Such an idealization permits a more logical mass treatment for the structure; that is, the mass of continuous sections is treated as continuous and all modes, including acoustic or organ-pipe modes, are present in the representation. Branches for representing the engine thrust structure and turbopumps were also incorporated. The parameter values for this model are presented in table V. This model was also altered to allow computation of the vibration modes of the vehicle with the guidance section removed.

Method of Solution

The lumped-mass-spring models of the Thor vehicle given in tables III and IV represent undamped, multidegree-of-freedom systems. The free-vibration equation associated with these analytical models is

$$[M]\{\ddot{y}\} + [K]\{y\} = \{0\} \tag{1}$$

where

$[M]$ square mass matrix

$[K]$ square stiffness matrix

$\{y\}$ column matrix of displacement vector

The analytical solution of equation (1) yields the natural frequencies and modes of the vehicle. The solution leads to the algebraic equation (ref. 8)

$$\left[K - \omega^2 M\right]\{Y\} = \{0\} \tag{2}$$

where $\{Y\}$ is a column matrix of unknown amplitude and ω is an unknown frequency. For nontrivial solutions of equation (2), it is necessary that the determinant of the matrix multiplying the vectors be zero; that is,

$$\det\left[K - \omega^2 M\right] = 0 \tag{3}$$

A digital computer program which utilizes a Jacobi diagonalization technique was used to obtain the solutions to equations (2) and (3) with the $[K]$ and $[M]$ matrices as input. An example of the matrices $[M]$ and $[K]$ for the 8-mass model is given in equations (4) and (5) in U.S. Customary Units for the data contained in table III.

$$M = \begin{bmatrix} 0.67 & & & & & & & \\ & 1.64 & & & & & & \\ & & 1.35 & & & & & \\ & & & 1.15 & & & & \\ & & & & 2.43 & & & \\ & & & & & 1.00 & & \\ & & & & & & 1.45 & \\ & & & & & & & 3.31 \end{bmatrix} \tag{4}$$

and

$$K = 10^6 \begin{bmatrix} 1.760 & -1.760 & & & & & & \\ -1.760 & 2.760 & -1.000 & & & & & \\ & -1.000 & 6.540 & -5.540 & & & & \\ & & -5.540 & 6.406 & -0.866 & & & \\ & & & -0.866 & 6.626 & -5.76 & & \\ & & & & -5.76 & 6.476 & -0.320 & -0.396 \\ & & & & & -0.320 & 0.320 & 0 \\ & & & & & -0.396 & 0 & 0.396 \end{bmatrix} \tag{5}$$

The determination of the modes, natural frequencies, and response levels of the Thor vehicle by means of the continuous-model representation (fig. 9) required the use of a different analysis technique than the method used for the lumped-mass models. The concept of receptance (sometimes called displacement mobility) was utilized to obtain the solution in this case. A more detailed discussion of the receptance method is presented in the appendix and in reference 6. In the receptance technique, the structural elements of the Thor were replaced with uniform bars as discussed in the previous section. Once the model had been formulated, the displacements at given locations were written in terms of the receptances of each vehicle subsection. (See appendix.) Displacement compatibility and force equilibrium were established as the complete system was synthesized from the various subsections. A matrix equation was then formulated from the resulting transcendental equations. A digital computer program was utilized to solve the matrix equation for the corresponding displacements and forces for a range of frequencies to obtain the variation of the response with frequency for the model. Frequencies at which the value of the determinant of the transcendental matrix is zero are the natural frequencies of the continuous model.

PRESENTATION OF EXPERIMENTAL DATA

Results of tests of the simplified, unpressurized Thor vehicle are presented in figures 10 to 13. Included in the results are the longitudinal frequency responses of the vehicle presented as input impedances for three conditions of the propellant tanks (see "Experimental Procedure") and as transfer impedances in missile bays A and B (see table II). Longitudinal modes, natural frequencies, and the acoustic responses of the two propellant tanks as well as the structural damping are also presented.

Modes and Frequencies

Normalized experimentally determined longitudinal modes of the vehicle are presented in figure 10. The mode shape was determined by normalizing the acceleration values along the vehicle with respect to the maximum values at the top (guidance section) of the vehicle. The three data points at $x/L = 0.081$ and 0.125 are measurements taken on the apex and the base of two of the thrust frame struts of the engine mass. (See table II.) The amplitudes compared with values on the basic vehicle structure nearby indicated that the engine and associated equipment masses were responding as branched or parallel masses to the vehicle structure. Figure 10(e) presents the normalized first longitudinal mode of the Thor with the guidance section removed. The removal of the guidance section (approximately 10 percent of the total mass) increased the first natural longitudinal frequency from 55.0 cps to 55.7 cps.

Forced-Vibration Response Data

Typical longitudinal response data of the simplified, unpressurized Thor vehicle are given in figures 11 to 13. The data of these figures are presented as input and/or transfer impedance. The input or driving point impedance is defined as the complex ratio of the driving force on a system to the resulting velocity at that point. Transfer impedance is defined as the complex ratio of the driving force to the velocity at another point. The complex ratio implies a phase relationship between the force and velocity; however, the impedance results presented herein are peak values, that is, no phase measurements were made during the tests. Peaks on the impedance curve indicate frequencies at which large forces are required to produce significant motion. Dips indicate resonant frequencies at which large motions may be obtained with small forces. Frequency regions where the impedance curve has a constant slope of +1 indicate mass-controlled action. Similarly, regions of the curve with a slope of -1 indicate spring-controlled action. At the frequencies of the peaks and dips, the impedance is limited by damping. Impedance data reported herein were obtained by taking the ratio of the measured input force to the accelerations in g units and plotting that ratio against frequency

on impedance plots. More detailed discussions of the mechanical impedance concept may be found in references 9 and 10.

Input impedance.- Presented in figure 11 is the input impedance at the apex of the thrust frame (station 667.7 or $x/L = 0.08$) or the shaker attachment point for the condition of closed fuel tank and LOX tank containing unpressurized air. The solid line of the figure represents the impedance for an input force of ±500 pounds (2224 N) while the open circles represent the impedance for an input force of ±900 pounds (4003 N). The results indicate that in the force range of the investigation, the response of the structure was apparently linear. At the low frequencies from approximately 5.0 cps to 20.0 cps, the vehicle was essentially a masslike structure; hence the +1 slope for the impedance along the mass line of approximately 5000 pounds (2270 kg) corresponds to the static mass of the missile. The first positive peak (antiresonance) occurred at about 25 cps, whereas the first longitudinal structural resonance occurred at 55.0 cps. The frequency range, however, did not encompass the second apparent major structural resonance (indicated by the dashed curve around 168.0 cps) as did subsequent tests. Because of the complexity of the structure many resonances also occurred between the longitudinal structural resonances of 55 and 168 cps as evidenced by the numerous peaks and dips between 55.0 cps and 168.0 cps in the figure. Those peaks which were investigated in some detail are indicated in figure 11 by the numbers that identify the resonant frequencies. Within the scope of the present investigation, no attempt was made to pinpoint the sources of the additional resonances; however, it is probable that local panel and/or shell resonances, or resonances of certain concentrated masses remaining on the vehicle contributed to many of the responses. The figure shows that below the first structural mode, identified at 55.0 cps, two resonant frequencies also existed at 27.7 cps and 34.0 cps. Further tests with the vehicle to identify these resonances are discussed in the following section.

Acoustic modes.- Tentative identification of the two strong, lightly damped resonances at 27.7 cps and 34.0 cps as acoustic modes was obtained by the use of the frequency equation for the vibration of an organ pipe or air column (ref. 11). The fundamental frequency for the LOX tank was calculated to be 28.0 cps whereas the fuel tank fundamental was 35.0 cps. Experimental studies were conducted to provide additional verification that these resonances were acoustic responses. Firstly, in an attempt to eliminate the responses, large vents were made in the top and bottom of the fuel tank by removing access plates and inlet covers, and three small vents were opened in the top of the LOX tank. A typical plot of the input impedance for these tank conditions is presented in figure 12. It may be seen that the resonance at 34.0 cps was eliminated by the venting of the fuel tank; however, the limited venting in the LOX tank was not sufficient to eliminate the resonance at 27.7 cps. Secondly, the fuel tank was left vented and the speed of sound of the acoustic medium in the LOX tank was increased by introducing a

volume of helium sufficient to give a mixture by volume of approximately 50-percent helium and 50-percent air. The input impedance for this case is presented in figure 13(a). In this figure, as in figure 11, regions of apparent major resonances are indicated by the approximate frequency at which they occur. Furthermore, this figure indicates the presence of four rather than two major structural resonances. The resonance at 27.7 cps was not noted; however, a resonance did occur at approximately 40 cps. Calculations of the velocity of sound for the gas mixture (ref. 12) gave an increase of 1.4 times the velocity of sound in air. Such a factor would increase the 27.7 cps frequency to about 39 cps which is approximately the experimentally observed shift. It was concluded from these results that the frequency of 27.7 cps was associated with the resonance of the air column in the LOX tank whereas the 34.0 cps frequency corresponded to the fuel-tank air-column resonance. No additional or observable changes were noted for the other resonant frequencies; thus there was little or no coupling with structural modes. Therefore, although the effects of the acoustic resonances on structural response may be appreciable, these effects are generally limited to a narrow band of frequencies near the acoustic resonances. Reference 13, which presents the results of an analytical and experimental study of several coupling phenomena involving the structure, the fluid, and the acoustic properties of some tank volumes, shows similar effects.

Transfer impedance.- Figures 13(b), 13(c), and 13(d) show typical transfer impedance data for the vehicle in bays A and B (see table II) at the top of the LOX tank ($x/L = 0.519$), the top of the fuel tank ($x/L = 0.840$), and the top of the guidance section ($x/L = 1.00$), respectively. The data in these figures are for the configuration with the fuel tank fully vented and with the LOX tank containing 50 percent helium closed and unpressurized. The four major structural resonances in the frequency range of the investigation as well as the additional resonances previously noted were also indicated in the transfer impedance at the various sections. In general, the transfer impedance levels in the region of masslike action were slightly lower than the input impedance level but approached the input level in trend. Since the vehicle is far from being an ideal system and some compliance or spring effect is inherent in all elements, it is possible that the vehicle suffered some deformation with motion even at the lower frequencies. Furthermore, any motion which might have occurred in the radial or circumferential directions could indicate increased motions to the transducers and thus lower values of impedance or apparent weight. The reductions of impedance were more noticeable at locations approaching the top of the vehicle.

Structural Damping

Structural damping determined by the log-decrement method is presented in table VI for the 55 and 168 cps longitudinal modes. These modes were selected because they were the most prominent and easily defined structural modes of the vehicle. The

values of damping are expressed in terms of the critical damping ratio C/C_c which is defined as

$$\frac{C}{C_c} = \frac{1}{2\pi n} \log_e \frac{Y_o}{Y_n}$$

where n is the number of cycles over which the decay was measured, Y_o is the initial amplitude, and Y_n is the amplitude after n cycles of oscillation. The data show that the damping ratio C/C_c is approximately 0.025 and 0.033 for the resonant frequencies of 55 cps and 168 cps, respectively. Two levels of force input were used in determining the damping in the 55 cps mode; however, the damping ratio was the same for each force level. Only one force level was then used in obtaining C/C_c for the 168 cps mode. The values of the damping ratio fall within the range of measured values for the Thor in lateral vehicle modes (ref. 14).

RESULTS AND DISCUSSION

Comparison of Experimental and Analytical Results

The mode shapes and frequencies for the complete Thor vehicle computed for both the lumped-mass and continuous analytical models and the input impedance (frequency response) computed for the continuous model are compared with the experimental results in this section. Also, the first mode computed for the configuration without the guidance section by using the lumped-mass and continuous analytical models of this report and also by the method of reference 7 are compared with the experimentally determined first mode of this configuration. The comparisons of experimental data with the analytical results are presented in figures 14 and 15 and table VII.

Mode shapes and frequencies.- A comparison of the analytically and experimentally determined mode shapes and associated natural frequencies is given in figure 14 and a summary of the ratios of experimental and analytical natural frequencies is given in table VII. The turbopump vibration response was not experimentally determined and therefore is not plotted in figure 14. Originally the turbopump and the thrust frame were not thought to contribute significantly (other than as rigid mass attachments) to the dynamic response of the vehicle in the frequency range containing the first two or three structural modes; however, when excited individually, their resonant frequencies were found to be approximately 75 cps and 55 cps, respectively. The analytical models therefore incorporate the turbopump and thrust structure as spring-mass attachments by including the parameter values given in tables III, IV, and V.

In figures 14(a) to (d) the first four structural modes of the vehicle predicted by the analytical models are compared with four corresponding experimental modes as indicated in figures 10(a) to (d). As already stated, there are no points for the turbopump in the

experimental modes. The mode shapes are all normalized with respect to the motion at the tip of the vehicle. The largest discrepancy in the mode shapes is for the motion of the apex (gimbal point) of the thrust cone in figures 14(a), (c), and (d); however, in figure 14(b) this comparison reveals nearly perfect agreement. Both analytical models predict nearly identical results. The agreement between the analytical and experimental results is considered to be quite satisfactory.

In figure 14(e) the mode shape and natural frequency are presented for the Thor without the guidance section. These studies were made to obtain quantitative information on the effect of changing the upper mass on vehicle response. The agreement for this case between analysis and experiment is fair.

The ratios of experimental to analytical natural frequencies presented in table VII indicate that the average difference between experiment and analysis is less than 3 percent, with no observable trends associated with either the higher or lower modes, or the method of analysis.

Forced vibration response.- The input impedance was computed using the continuous model and is compared with the experimentally determined input impedance (fig. 11) and transfer impedance (fig. 13(d)) in figure 15. The acoustic as well as structural responses are predicted by the continuous model; however, only the fundamental acoustic responses are shown in figure 15(a) and none in 15(b). In addition to predicting the natural frequencies of the vehicle (experimental values indicated on the figure) the overall response level predicted by the analysis appears to be satisfactory which is a qualitative indication that the analytical model is satisfactory.

Use of turbopump and thrust structure data.- It should be noted that the analytical results presented in this report were obtained only after the turbopump and thrust frame were incorporated in the analytical models as branches tuned to their respective uncoupled experimental frequencies. Preliminary analyses, which either ignored these components or incorporated them by using spring rates computed from drawings and specifications of the structure, were unsatisfactory.

Discussion of Results

The analytical models presented in this report included the turbopump and thrust frame as spring-mass branches and the vibration characteristics of these branches were experimentally determined by separate tests for incorporation in the analysis. The resulting analytical models predicted resonant frequencies which were in good agreement with the data presented in figures 11 and 13(a) which indicate the existence of six major vehicle resonances at frequencies of approximately 27.7, 34, 55, 68, 113, and 168 cps. However, there are also many other resonant modes of the vehicle in this range of frequencies and there are other spring-mass attachments such as the fuel transfer tube and

nitrogen spheres which could also be included, if desired, with the possibility of achieving slightly better agreement between the experimental and analytical results.

Of the two analytical techniques used in the present study (that is, lumped mass-spring and continuous analytical models), there was no apparent improvement in predicted results by the use of a continuous one-dimensional representation of the Thor vehicle over the results of the lumped mass-spring results. This result is, perhaps, an expected one since any inadequacy in the knowledge of structural properties and in the data used in the input for the lumped mass-spring representations would also be reflected in the input to the continuous-model representation. In contrast to the lumped mass-spring analysis, however, the continuous model included the acoustic or organ-pipe modes, and the results of the analysis with the continuous model indicated that the acoustic modes of the LOX and fuel tanks did not strongly couple with the structural responses. The main influence of the acoustic resonances on the structural characteristics was generally limited to a narrow band of frequencies near the acoustic resonances. The experimental results also verified that little or no coupling of the acoustic responses with the structural modes occurred.

Although the empty, unpressurized, simplified Thor is not a realistic flight vehicle, it does possess all of the essential components of a launch vehicle structure. Investigation of its vibration response serves a useful research purpose in helping to modify and verify analytical procedures and to provide much needed insight into the analysis of complex structures.

CONCLUSIONS

An experimental and analytical investigation has been conducted of the longitudinal vibration of a simplified Thor vehicle structure. The results and conclusions are summarized in the following paragraphs.

1. Input and transfer impedance results for the Thor vehicle indicated the existence of six major resonances in the frequency range from approximately 5.0 cps to 200.0 cps. A large number of secondary resonances between 55.0 cps and 168.0 cps were also indicated by the impedance data.

2. The results indicate that in the force range of the investigation, the structure responded linearly.

3. Two of the strong lightly damped and highly tuned resonances noted on the structure were identified as the fundamental acoustic or organ-pipe modes of the empty LOX and fuel tanks. The LOX tank acoustic resonances were identified at 27.7 cps whereas the fuel-tank acoustic mode was noted at 34.0 cps. The experimental and analytical

results indicated that the acoustic mode response was generally limited to a very narrow frequency band. No observable coupling with the structural modes was indicated in this case.

4. Of two different one-dimensional analytical models that were devised, both predicted natural frequencies, mode shapes, and input and transfer impedance characteristics which are in excellent agreement with the experimental results.

5. Vibration tests of the full-size vehicle including the determination of the uncoupled natural frequencies of branched spring-mass systems were required in order to achieve an analytical model which was dynamically equivalent to the actual vehicle.

6. A comparison of the results of the lumped mass-spring and the continuous models indicates no apparent improvement in analytical results by the use of a one-dimensional continuous representation of the Thor over the use of a one-dimensional lumped mass-spring representation.

Langley Research Center,
National Aeronautics and Space Administration,
Langley Station, Hampton, Va., December 21, 1965.

APPENDIX

RECEPTANCE METHOD

This appendix is included to present briefly information required in utilizing the concept of receptance (sometimes called displacement mobility) for calculating the mode shapes, resonant frequencies, and response levels of the one-dimensional continuous analytical model representation of the Thor vehicle.

Basis of Method

If an undamped linear system is subjected to a simple harmonic force $F_l e^{j\omega t}$ acting at point l, the steady response of point k may be written

$$y_k = \alpha_{kl} F_l e^{j\omega t} \tag{A1}$$

where α_{kl}, the receptance, is defined as the steady response at point k due to the application of a simple harmonic force of unit amplitude at point l. It is clear that α_{kl} is, in general, a function of the driving frequency ω. The steady forced amplitude is given by

$$Y_k = \alpha_{kl} F_l \tag{A2}$$

When α_{kl} is negative, the phase angle between the response and forcing function is an odd multiple of 180^o. For example, the receptance for a mass element is

$$\alpha = \frac{-1}{M\omega^2} \tag{A3}$$

and for a spring element the receptance is

$$\alpha = \frac{1}{K} \tag{A4}$$

As an example for a slightly more complicated system, the receptance for a mass element attached to the free end of a spring can be derived by using suitable compatability relations.

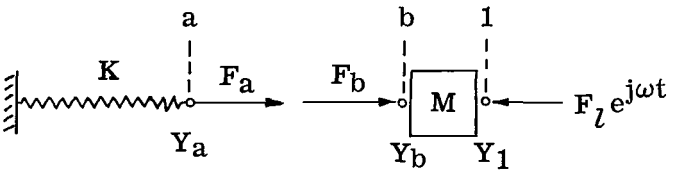

At point 1,

$$\left.\begin{aligned} y_a = y_b = y_1 \\ Y_a = Y_b = Y_1 \end{aligned}\right\} \tag{A5a}$$

or

and

$$F_a + F_b = F_1 \tag{A5b}$$

APPENDIX

From equations (A2), (A3), and (A4), the amplitude of the response is

$$Y_a = \frac{1}{K} F_a \tag{A6}$$

$$Y_b = -\frac{1}{M\omega^2} F_b \tag{A7}$$

$$Y_1 = \alpha_{11} F_1 \tag{A8}$$

Solving equations (A6), (A7), and (A8) for force and substituting into equation (A5b)

$$KY_a - M\omega^2 Y_b = \frac{Y_1}{\alpha_{11}} \tag{A9}$$

and using the relationship of equation (A5a)

$$\left(K - M\omega^2\right) Y_1 = \frac{Y_1}{\alpha_{11}} \tag{A10}$$

gives

$$\alpha_{11} = \frac{1}{K - M\omega^2} \tag{A11}$$

as the receptance for a spring-mass element.

Application to Test Vehicle

The rules for obtaining the receptance of combined subsystems (for which the individual subsystem receptances are known) may be deduced very readily from the approach outlined or from the fully developed approach in reference 8; however, as an aid to the reader, the equations for the LOX tank and center-body sections of the Thor are written as follows (see also fig. 9):

For the LOX tank section:

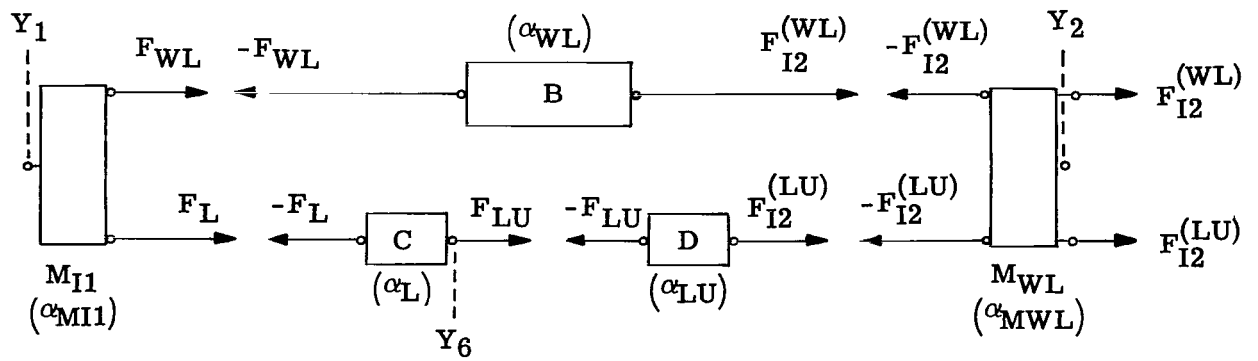

$$Y_1 = -F_L\alpha_{L,11} + F_{LU}\alpha_{L,16} \tag{A12a}$$

$$Y_1 = -F_{WL}\alpha_{WL,11} + F_{I2}^{(WL)}\alpha_{WL,12} \tag{A12b}$$

$$Y_6 = -F_L\alpha_{L,61} + F_{LU}\alpha_{L,66} \tag{A13a}$$

$$Y_6 = -F_{LU}\alpha_{LU,66} + F_{I2}^{(LU)}\alpha_{LU,62} \tag{A13b}$$

$$Y_2 = -F_{LU}\alpha_{LU,26} + F_{I2}^{(LU)}\alpha_{LU,22} \tag{A14a}$$

$$Y_2 = -F_{WL}\alpha_{WL,21} + F_{I2}^{(WL)}\alpha_{WL,22} \tag{A14b}$$

For the center-body section:

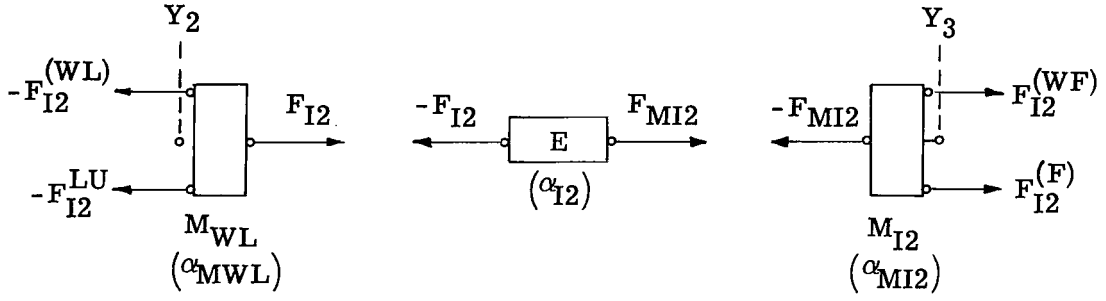

$$Y_2 = \left[-\left(F_{I2}^{(WL)} + F_{I2}^{(LU)}\right) + F_{I2}\right]\alpha_{MWL} \tag{A15a}$$

$$Y_2 = -F_{I2}\alpha_{I2,22} + F_{MI2}\alpha_{I2,23} \tag{A15b}$$

$$Y_3 = -F_{I2}\alpha_{I2,32} + F_{MI2}\alpha_{I2,33} \tag{A16a}$$

$$Y_3 = \left[-F_{MI2} + F_{I2}^{(WF)} + F_{I2}^{(F)}\right]\alpha_{MI2} \tag{A16b}$$

The receptances appearing in equations (A12) to (A16) and in the additional equations for the remaining sections of the continuous analytical model (fig. 9) are as follows:

$$\alpha_E = -\frac{1}{M_E\omega^2} \tag{A17}$$

APPENDIX

$$\alpha_{F,77} = \alpha_{F,37} = \alpha_{F,73} = \frac{-1}{M_F\omega^2} \tag{A18a}$$

$$\alpha_{F,33} = \frac{-\left(K_F - M_F\omega^2\right)}{K_F M_F \omega^2} \tag{A18b}$$

$$\alpha_{G,44} = \alpha_{G,55} = \frac{-\cos\left(\lambda_G L_G\right)}{A_G E \lambda_G \sin\left(\lambda_G L_G\right)} \tag{A19a}$$

$$\alpha_{G,45} = \alpha_{G,54} = \frac{-1}{A_G E \lambda_G \sin\left(\lambda_G L_G\right)} \tag{A19b}$$

$$\alpha_{I1,00} = \alpha_{I1,11} = \frac{-\cos\left(\lambda_{I1} L_{I1}\right)}{A_{I1} E \lambda_{I1} \sin\left(\lambda_{I1} L_{I1}\right)} \tag{A20a}$$

$$\alpha_{I1,01} = \alpha_{I1,10} = \frac{-1}{A_{I1} E \lambda_{I1} \sin\left(\lambda_{I1} L_{I1}\right)} \tag{A20b}$$

$$\alpha_{I2,22} = \alpha_{I2,33} = \frac{-\cos\left(\lambda_{I2} L_{I2}\right)}{A_{I2} E \lambda_{I2} \sin\left(\lambda_{I2} L_{I2}\right)} \tag{A21a}$$

$$\alpha_{I2,23} = \alpha_{I2,32} = \frac{-1}{A_{I2} E \lambda_{I2} \sin\left(\lambda_{I2} L_{I2}\right)} \tag{A21b}$$

$$\alpha_{LU,66} = \alpha_{LU,22} = \frac{-\cos\left(\lambda_{LU} L_{LU}\right)}{A_{LU} p_o k \lambda_{LU} \sin\left(\lambda_{LU} L_{LU}\right)} \tag{A22a}$$

$$\alpha_{LU,62} = \alpha_{LU,26} = \frac{-1}{A_{LU} p_o k \lambda_{LU} \sin\left(\lambda_{LU} L_{LU}\right)} \tag{A22b}$$

$$\alpha_{MI1} = \frac{-1}{M_{I1}\omega^2} \tag{A23}$$

$$\alpha_{MI2} = \frac{-1}{M_{I2}\omega^2} \tag{A24}$$

$$\alpha_{MWF} = \frac{-1}{M_{WF}\omega^2} \tag{A25}$$

$$\alpha_{MWL} = \frac{-1}{M_{WL}\omega^2} \tag{A26}$$

$$\alpha_{p} = \frac{-1}{M_{p}\omega^2} \tag{A27}$$

$$\alpha_{FU,77} = \alpha_{FU,44} = \frac{-\cos\left(\lambda_{FU}L_{FU}\right)}{A_{FU}p_{o}k\lambda_{FU}\sin\left(\lambda_{FU}L_{FU}\right)} \tag{A28a}$$

$$\alpha_{FU,74} = \alpha_{FU,47} = \frac{-1}{A_{FU}p_{o}k\lambda_{FU}\sin\left(\lambda_{FU}L_{FU}\right)} \tag{A28b}$$

$$\alpha_{L,16} = \alpha_{L,61} = \alpha_{L,66} = \frac{-1}{M_{L}\omega^2} \tag{A29a}$$

$$\alpha_{L,11} = \frac{-\left(K_{L} - M_{L}\omega^2\right)}{K_{L}M_{L}\omega^2} \tag{A29b}$$

A matrix equation for the completely synthesized continuous model of the Thor vehicle is constructed from the equations of force and displacement compatibility of the individual subsystems. Equations (A12) to (A16) are examples for the LOX tank section (subsystems B, C, and D) and the center-body section (subsystem E). The method of solution for the continuous model requires that the value of the matrix equation and the corresponding displacements and forces be computed for a range of frequencies to obtain the variation of response with frequency of the model. The frequencies at which the value of the determinant is zero are the natural frequencies of the continuous model.

A digital computer program specialized to this configuration was utilized to obtain the solutions given in table VII and figure 15 for the continuous model.

REFERENCES

1. Rosé, R. G.; and Simson, A. K.: A Study of System-Coupled Longitudinal Instabilities in Liquid Rockets. Special Report No. 1 – Analytic Model. AFRPL-TR-64-178, U.S. Air Force, Apr. 1965.

2. McKenna, K. J.; Walker, J. H.; and Winje, R. A.: Engine-Airframe Coupling in Liquid Rocket Systems. J. Spacecraft and Rockets, vol. 2, no. 2, Mar.-Apr. 1965, pp. 254-256.

3. Meltzer, E. C.: Compilation of Shock and Vibration Flight Data From Eight Thor-Related Vehicles. NASA CR-196, 1965.

4. Anon.: Thor Longitudinal Oscillation Study. Rept. SM-45009, Missile and Spacecraft Systems Division, Douglas Aircraft Company, Inc., Mar. 1964.

5. Davis, W. F.; Lynch, T. F.; and Murray, T. R.: Thor 20-Cycle Longitudinal Oscillation Study. The Shock and Vibration Bulletin, Bull. No. 34, Pt. 2, U.S. Dept. Defense, Dec. 1964, pp. 177-196. (Available from DDC as AD 460000.)

6. Bishop, R. E. D.; and Johnson, D. C.: The Mechanics of Vibration. Cambridge Univ. Press, c.1960.

7. Wood, John D.: Survey on Missile Structural Dynamics. 7102-0041-NU-000, EM 11-11 (BSD-TN-61-42) Space Technol. Lab., Inc., Los Angeles, California, 1 June 1961.

8. Harris, Cyril M.; and Crede, Charles E., eds.: Shock and Vibration Handbook. Vol. 2 – Data Analysis, Testing, and Methods of Control. McGraw-Hill Book Co., Inc., c.1961.

9. Harris, Cyril M.; and Crede, Charles E., eds.: Shock and Vibration Handbook. Vol. 1 – Basic Theory and Measurements. McGraw-Hill Book Co., Inc., c.1961.

10. Belsheim, R. O.; and Young, J. W., Jr.: Mechanical Impedance as a Tool for Shock or Vibration Analysis. Structures Branch, Mechanics Division. U.S. Naval Res. Lab., Washington, D.C., Feb. 15, 1960.

11. Hausman, Erich; and Slack, Edgar P.: Physics. Fourth ed., D. Van Nostrand Company, Inc., c.1957.

12. Jones, James B.; and Hawkins, George A.: Engineering Thermodynamics. John Wiley & Sons, Inc., c.1960.

13. Runyan, Harry L.; Pratt, Kermit G.; and Pierce, Harold B.: Some Hydro-Elastic-Pneumatic Problems Arising in the Structural Dynamics of Launch Vehicles. Paper presented at National Conference of Aviation and Space Division of ASME, Mar. 1965.

14. Eldred, K.; Roberts, W.; and White R.: Structural Vibrations in Space Vehicles. WADD Tech. Rep. 61-62, U.S. Air Force, Dec. 1961.

TABLE I.- WEIGHTS AND CENTER OF GRAVITY OF THOR COMPONENTS

Vehicle component	Experimental mass		Center-of-gravity locations (a)	
	lbm	kg	in.	m
Engine and accessory section	[b]1997	906	663.55	16.854
LOX tank	1402	636	------	------
Center body	198	89.8	351.70	8.933
Fuel tank	766	347	------	------
Guidance section	504	229	98.26	2.496
Transfer tube and insulation	134	60.8	------	------
Fuel, LOX tanks, and center body	2502	1135	426.80	10.841
Fuel tank and center body	964	437	------	------
Thor minus guidance section	4523	2052	532.70	13.531
Simplified unpressurized Thor	5029	2281	489.75	12.440

[a]Indicates vehicle stations. See figure 1 and/or table II.

[b]Expansion nozzle, gimbal, and some smaller items not included.

TABLE II.- INSTRUMENTATION LOCATIONS

[F refers to crystal force transducer; K refers to linear servo accelerometer]

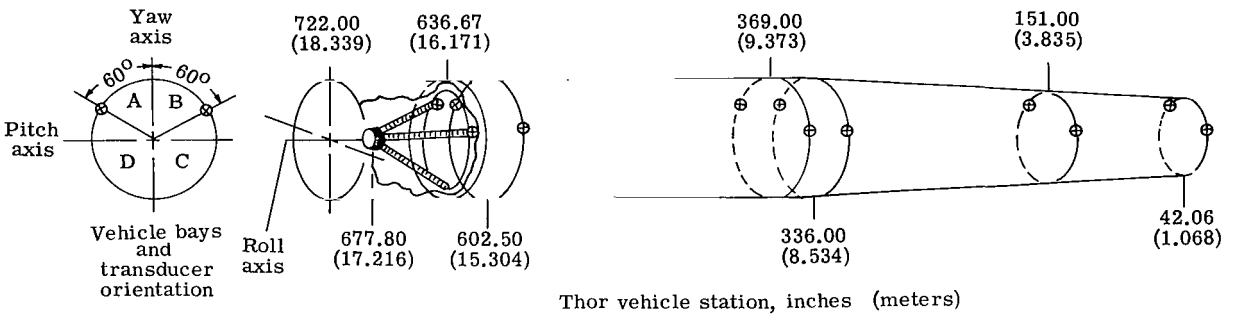

Transducer	Station	Bay	Missile structure
F-1	677.80 (17.216)	Vehicle roll axis	Apex of thrust frame
K-2	677.80 (17.216)	Vehicle roll axis	Apex of thrust frame
K-3	636.67 (16.171)	A	Top of thrust frame
K-4	636.67 (16.171)	B	Top of thrust frame
K-5	602.50 (15.304)	A	Bottom of LOX tank
K-6	602.50 (15.304)	B	Bottom of LOX tank
K-7	369.00 (9.373)	A	Top of LOX tank
K-8	369.00 (9.373)	B	Top of LOX tank
K-9	336.00 (8.534)	A	Bottom of fuel tank
K-10	336.00 (8.534)	B	Bottom of fuel tank
K-11	151.00 (3.835)	A	Top of fuel tank
K-12	151.00 (3.835)	B	Top of fuel tank
K-13	42.06 (1.068)	A	Top of guidance section
K-14	42.06 (1.068)	B	Top of guidance section

TABLE III.- AN 8-MASS ANALYTICAL MODEL OF THOR VEHICLE

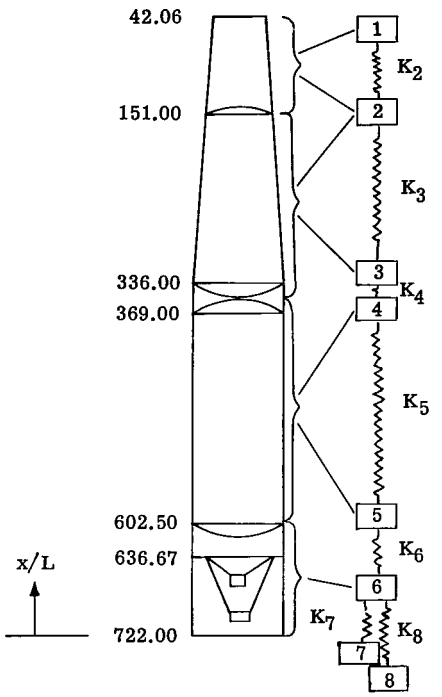

(a) U.S. Customary Units

Segment	x/L	Center of gravity, in.	Mass, lb-sec^2/in.	K, lb/in.
1	1.000	42	0.67	0
2	.840	151	1.64	1.760×10^6
3	.568	336	1.35	1.000
4	.519	369	1.15	5.540
5	.179	602	2.43	.866
6	.087	663	1.00	5.760
7	.106	650	1.45	.320
8	.100	654	3.31	.396

(b) International System of Units

Segment	x/L	Center of gravity, m	Mass, kg	K, MN/m
1	1.000	1.067	1.196	0
2	.840	3.835	2.929	308.2
3	.568	8.534	2.411	175.1
4	.519	9.373	2.054	970.2
5	.179	15.291	4.339	151.7
6	.087	16.840	1.780	1008.7
7	.106	16.500	2.591	56.1
8	.100	16.590	5.912	69.4

TABLE IV.- A 7-MASS ANALYTICAL MODEL OF THOR VEHICLE

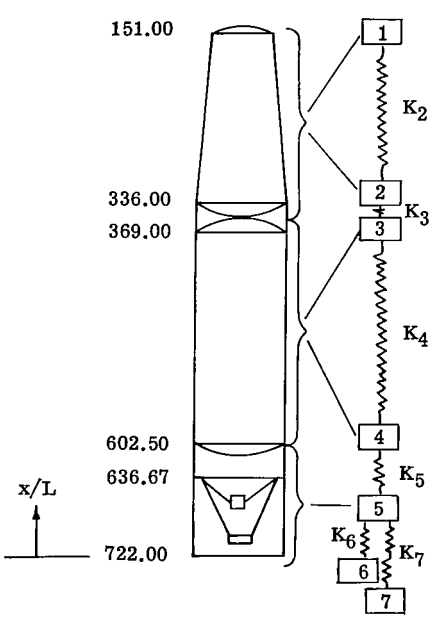

(a) U.S. Customary Units

Segment	x/L	Center of gravity, in.	Mass, lb-sec^2/in.	K, lb/in.
1	0.840	151	1.00	0
2	.568	336	1.35	1.000×10^6
3	.519	369	1.15	5.540
4	.179	602	2.43	.866
5	.087	663	1.00	5.760
6	.106	650	1.45	.320
7	.100	654	3.31	.396

(b) International System of Units

Segment	x/L	Center of gravity, m	Mass, kg	K, N/m
1	0.840	3.835	1.785	0
2	.568	8.534	2.929	1.751×10^8
3	.519	9.373	2.411	9.702
4	.179	15.291	4.339	1.517
5	.087	16.840	1.780	10.087
6	.106	16.500	2.591	.561
7	.100	16.590	5.912	.694

TABLE V.- INPUT DATA FOR CONTINUOUS MODEL ANALYTICAL REPRESENTATION OF THOR

Quantity	U.S. Customary Units	SI Units	Quantity	U.S. Customary Units	SI Units
A_G	19.2 in.^{2}	12.4 m^2	L_G	109 in.	2.77 m
A_{I1}	30.7 in.^{2}	19.8 m^2	L_{I1}	36 in.	0.91 m
A_{I2}	18.3 in.^{2}	11.7 m^2	L_{I2}	33 in.	0.84 m
A_L	7238 in.^{2}	4700 m^2	L_L	195 in.	4.95 m
A_{FU}	5281 in.^{2}	3407 m^2	L_{FU}	250 in.	6.35 m
A_{WF}	18.5 in.^{2}	11.9 m^2	L_{WF}	185 in.	4.70 m
A_{WL}	20.0 in.^{2}	12.9 m^2	L_{WL}	231 in.	5.87 m
a_G	196400 in./sec	4988 m/sec	M_E	0.95 lb-sec^2/in.	1.7 kg
a_{I1}	196400 in./sec	4988 m/sec	M_F	0.03 lb-sec^2/in.	0.0536 kg
a_{I2}	196400 in./sec	4988 m/sec	M_{I1}	1.74 lb-sec^2/in.	3.11 kg
a_L	13200 in./sec	335 m/sec	M_{I2}	0.83 lb-sec^2/in.	1.48 kg
a_{FU}	13200 in./sec	335 m/sec	M_L	0.03 lb-sec^2/in.	0.0536 kg
a_{WF}	196400 in./sec	4988 m/sec	M_p	0.40 lb-sec^2/in.	0.71 kg
a_{WL}	196400 in./sec	4988 m/sec	M_{TF}	3.26 lb-sec^2/in.	5.83 kg
E	10^7 lbf/in.^{2}	68900 MN/m^2	M_{TP}	1.45 lb-sec^2/in.	2.59 kg
$F_S(t)$	1 lbf	4.45 N	M_{WF}	0.933 lb-sec^2/in.	1.666 kg
K_F	1×10^6 lbf/in.	175 MN/m	M_{WL}	0.48 lb-sec^2/in.	0.86 kg
K_L	1×10^6 lbf/in.	175 MN/m	p_o	15 lbf/in.^{2}	10340 N/m^2
K_{TF}	0.396×10^6 lbf/in.	69.6 MN/m	γ	1.4	1.4
K_{TP}	0.32×10^6 lbf/in.	56.2 MN/m			

TABLE VI.- EXPERIMENTALLY DETERMINED DAMPING RATIOS

Force input		Resonant frequency, cps	Damping ratio, C/C_c
Pounds	Newtons		
200	890	55	0.0260
200	890	55	.0255
400	1779	55	.0254
400	1779	55	.0257
260	1157	168	.0330
260	1157	168	.0325
260	1157	168	.0328

TABLE VII.- SUMMARY OF RATIOS OF EXPERIMENTAL AND ANALYTICAL NATURAL FREQUENCIES

Frequency ratio	8-mass lumped	8-mass continuous
With guidance section		
$\frac{f_{1e}}{f_{1c}}$	$\frac{55}{55} \approx 1.00$	$\frac{55}{54.25} \approx 1.01$
$\frac{f_{2e}}{f_{2c}}$	$\frac{68.1}{69.6} \approx 0.97$	$\frac{68.1}{69.8} \approx 0.97$
$\frac{f_{3e}}{f_{3c}}$	$\frac{112.9}{111} \approx 1.02$	$\frac{112.9}{114.3} \approx 0.99$
$\frac{f_{4e}}{f_{4c}}$	$\frac{168}{166} \approx 1.01$	$\frac{168}{156} \approx 1.08$
Guidance section removed		
$\frac{f_{1e}}{f_{1c}}$	$\frac{55.7}{59} \approx 0.95$	$\frac{55.7}{57} \approx 0.98$

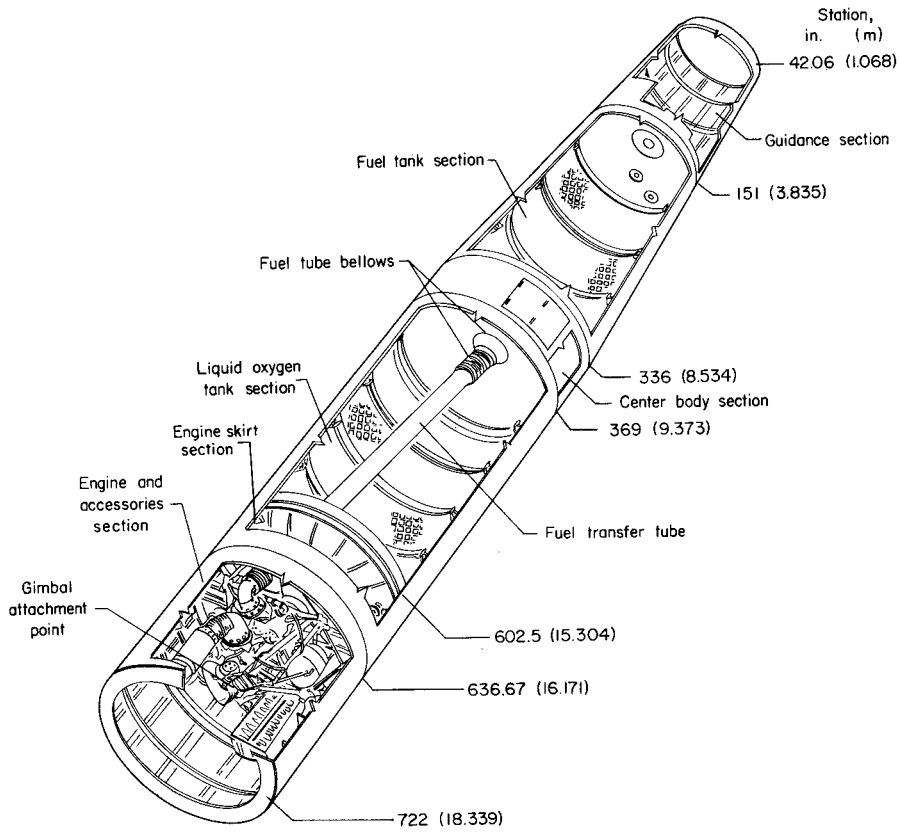

(a) Schematic cut-away of Thor.

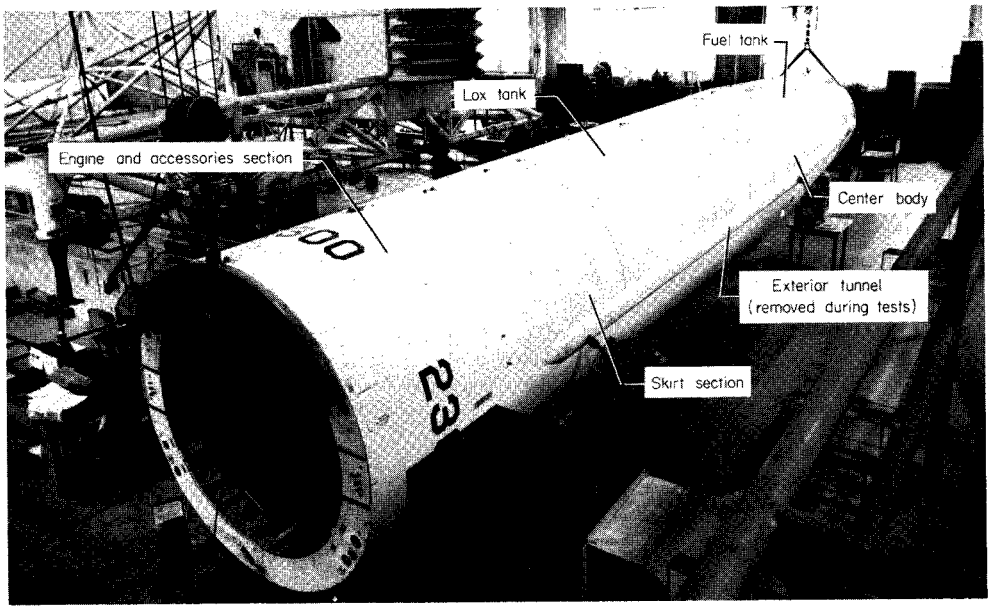

(b) Assembled vehicle (no guidance section). L-65-1727.1

Figure 1.- Thor vehicle airframe.

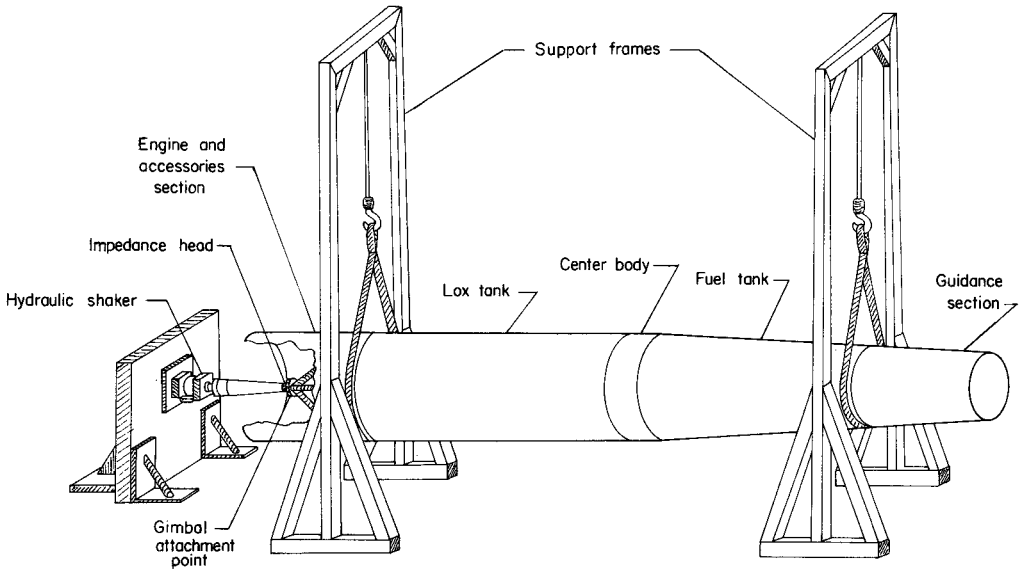

Figure 2.- Thor launch vehicle test setup.

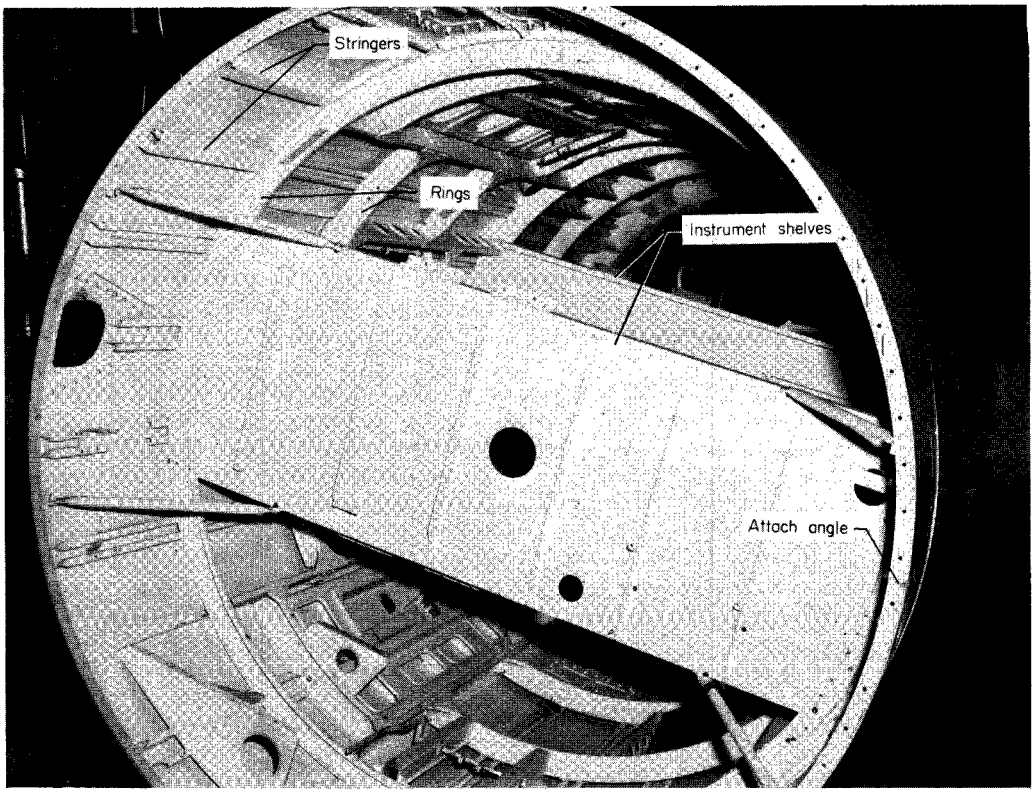

Figure 3.- Interior of Thor guidance section. L-64-9950.1

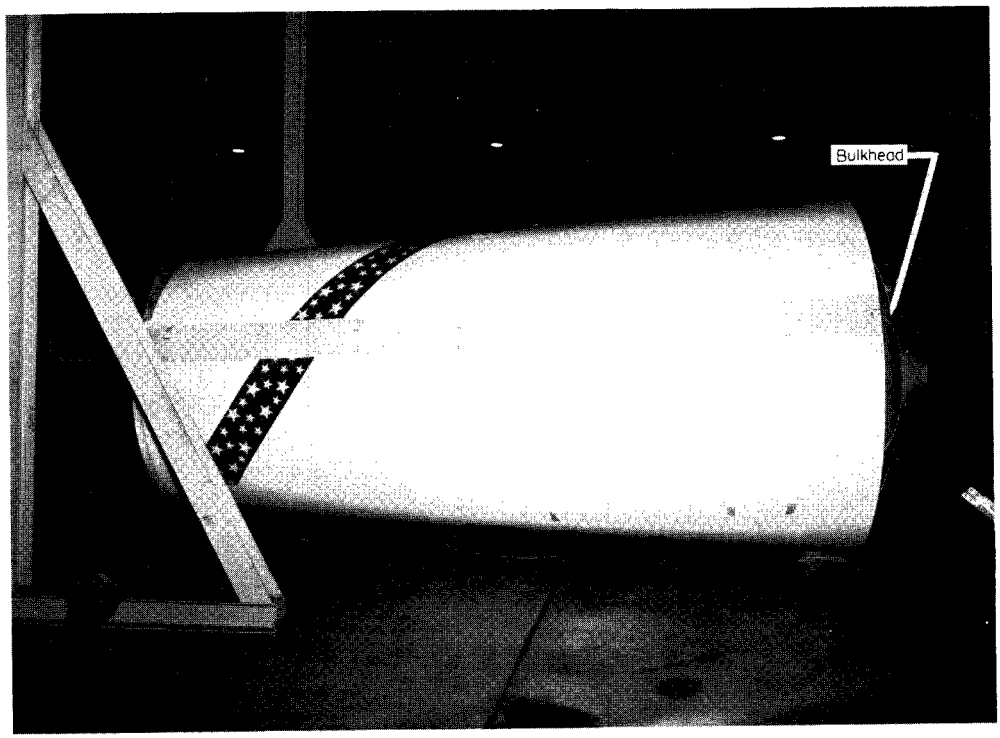

Figure 4.- Thor fuel tank section. L-64-9486.1

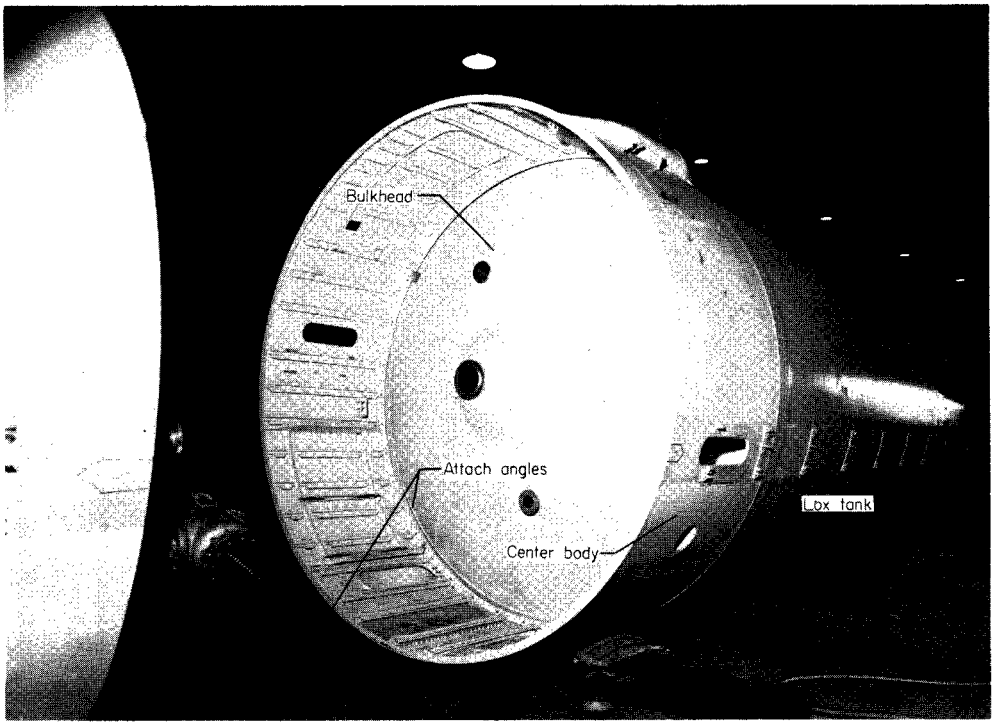

Figure 5.- Thor center body and LOX tank sections. L-64-7308.1

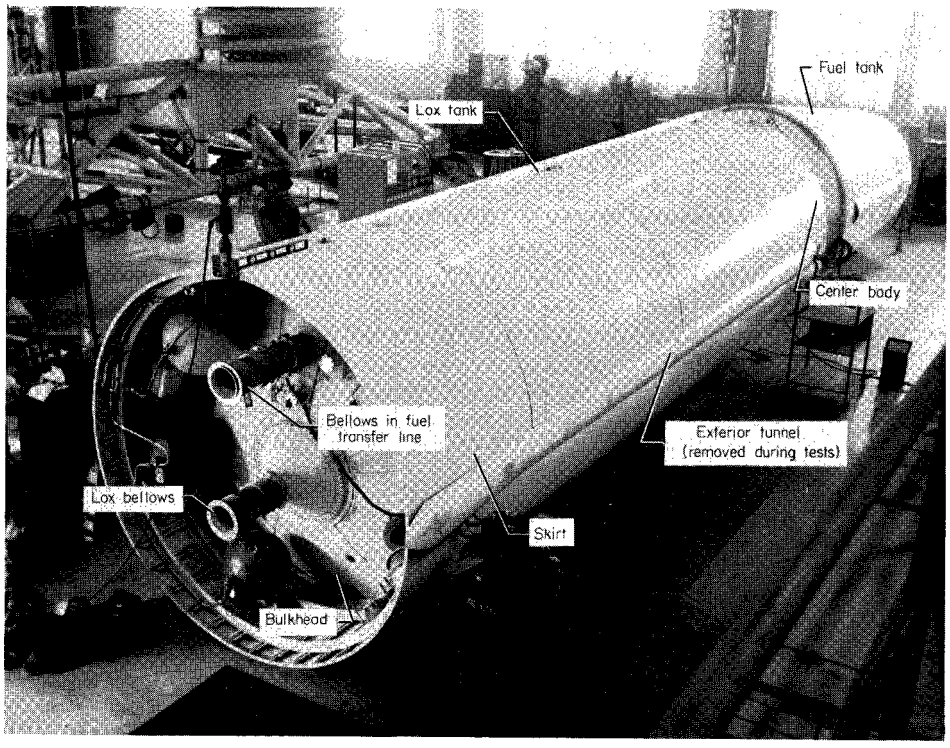

Figure 6.- Fuel tank, center body, LOX tank, and skirt sections. L-65-1422.2

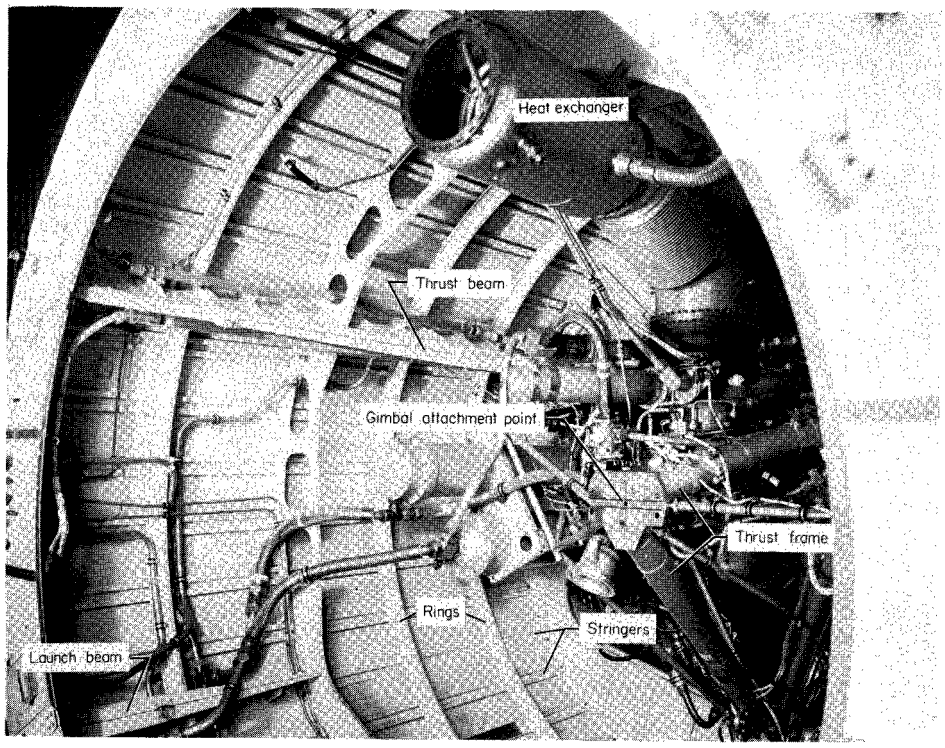

Figure 7.- Interior of engine and accessories section. L-64-6375.2

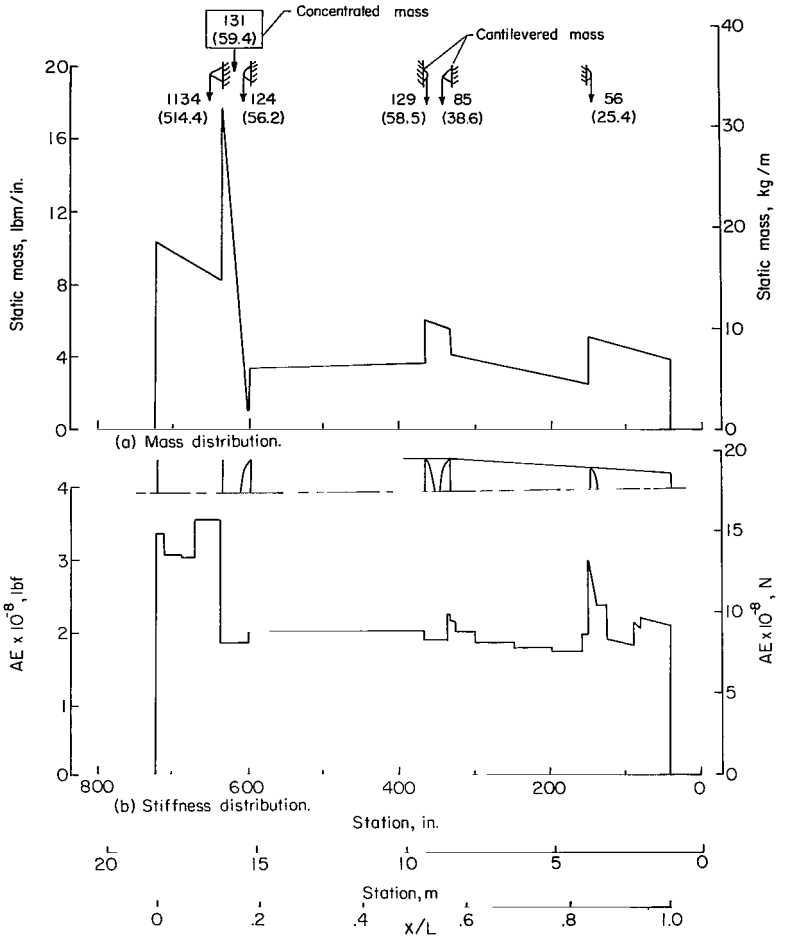

Figure 8.- Mass and stiffness distribution for empty Thor.

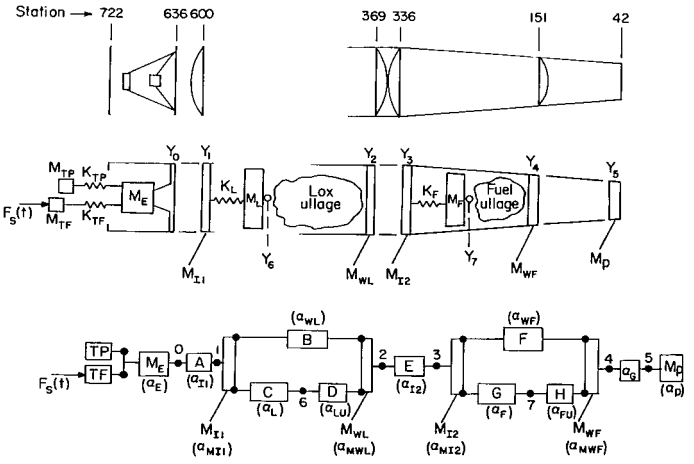

Figure 9.- Continuous-model analytical representation and receptance diagram for Thor.

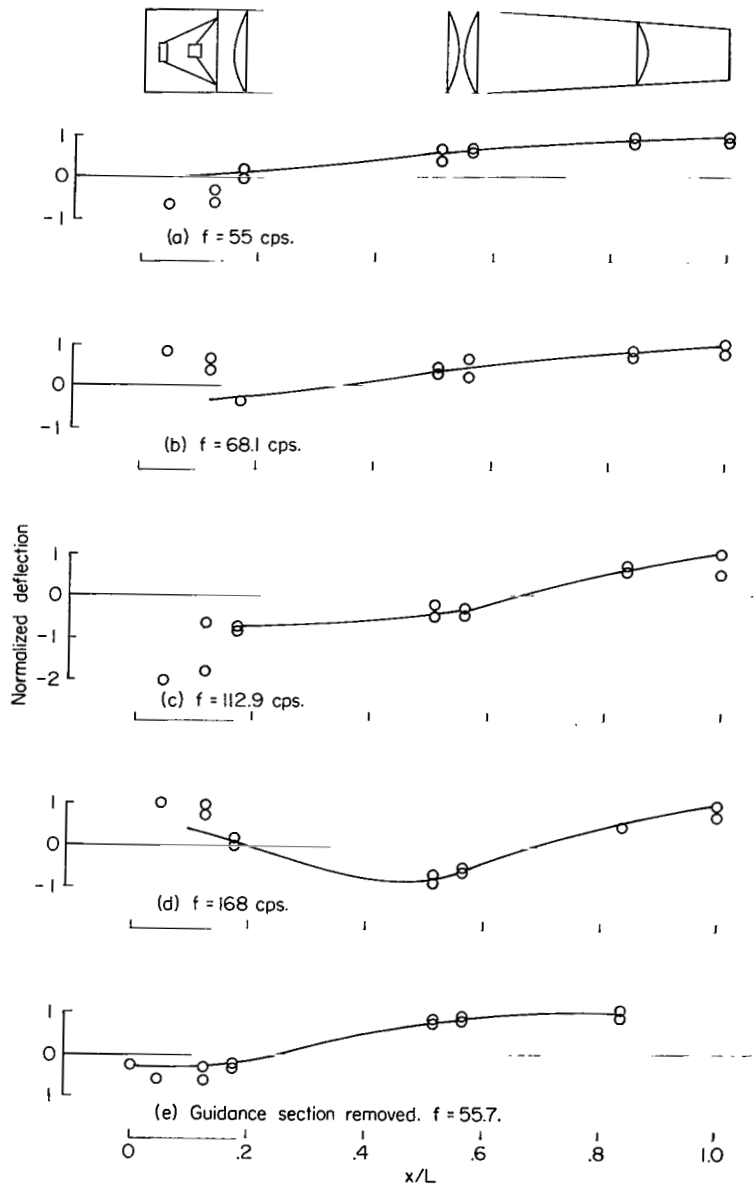

Figure 10.- Experimental longitudinal free-free modes and frequencies of the Thor vehicle.

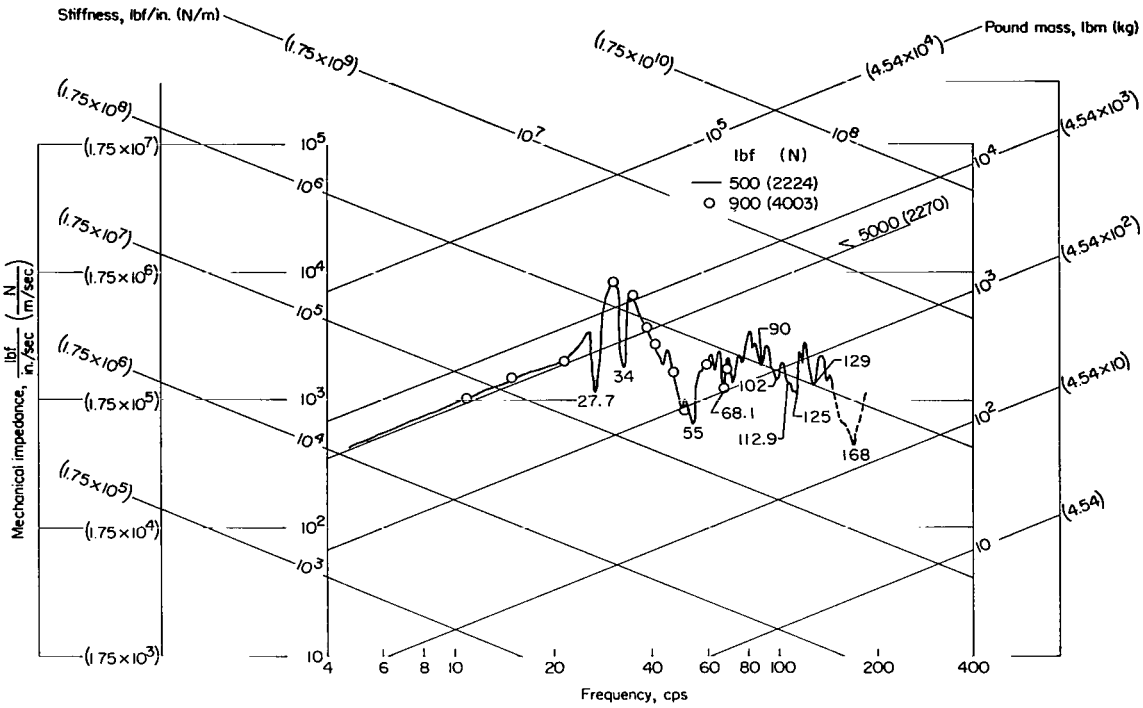

Figure 11.- Longitudinal input impedance at the gimbal point of Thor vehicle. LOX and fuel tanks closed and unpressurized.

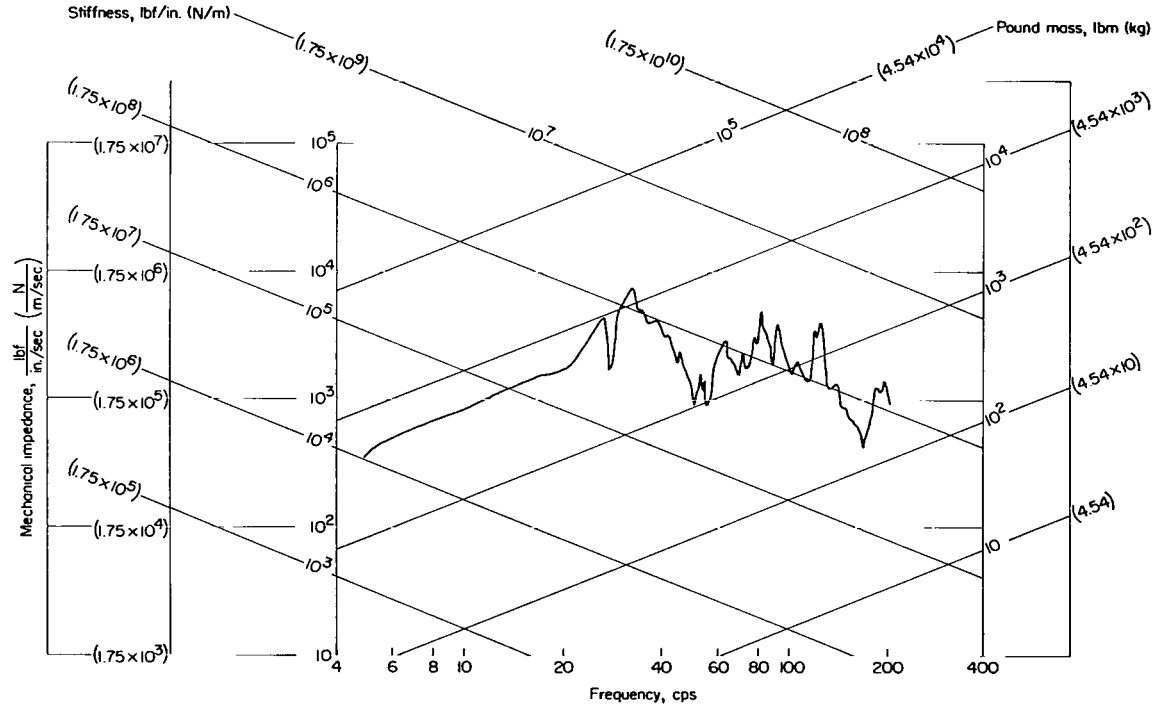

Figure 12.- Longitudinal input impedance at the gimbal point of Thor vehicle. Fuel tank fully vented, LOX tank partially vented.

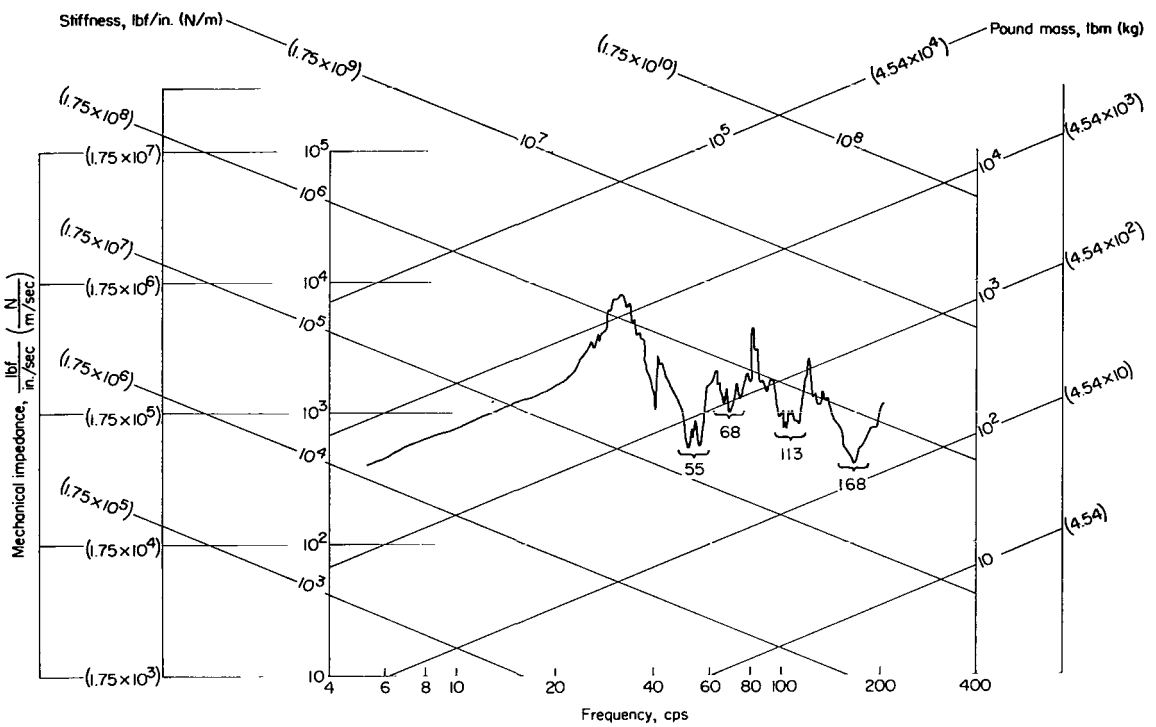

(a) Longitudinal input impedance at gimbal point.

Figure 13.- Longitudinal impedance of Thor vehicle. Fuel tank fully vented, LOX tank closed-unpressurized containing 50 percent by volume He-air mixture.

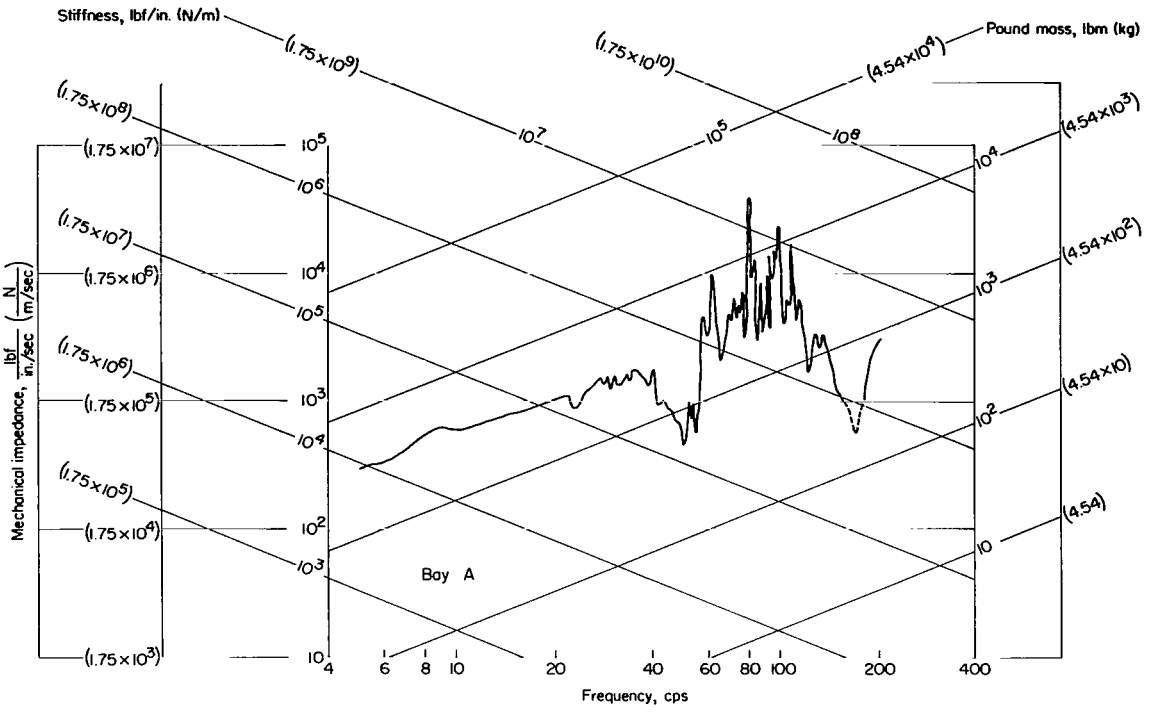

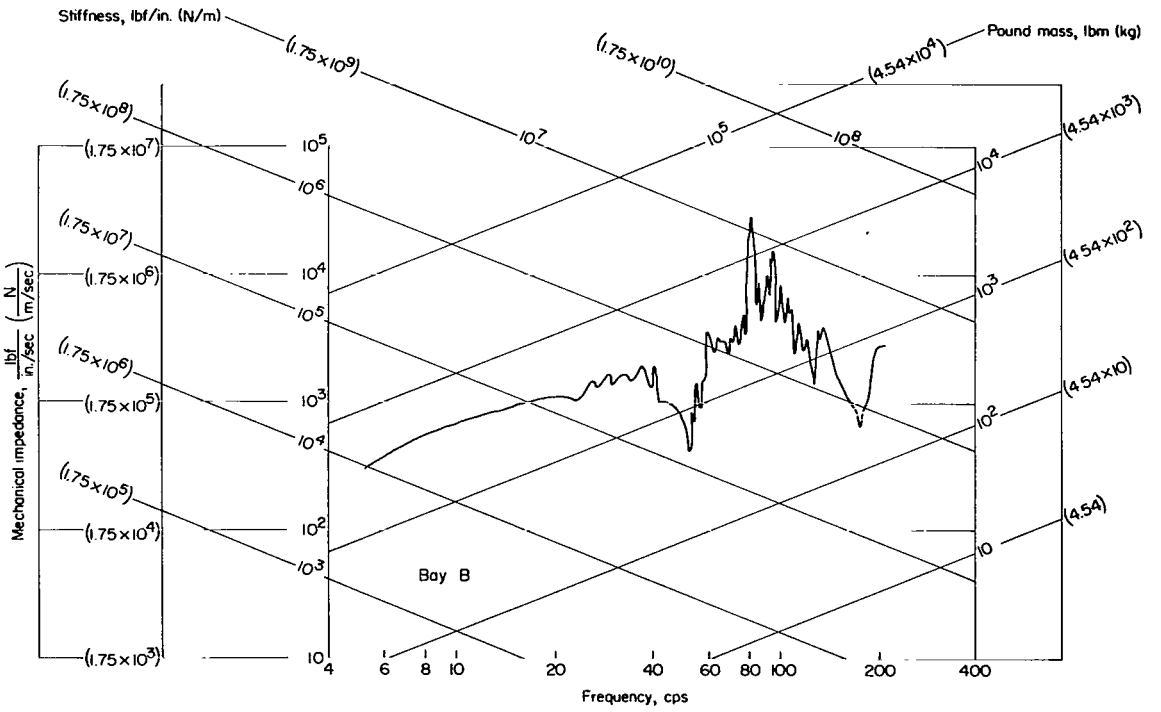

(b) Longitudinal transfer impedance at top of LOX tank in bays A and B. Force input at gimbal point.

Figure 13.- Continued.

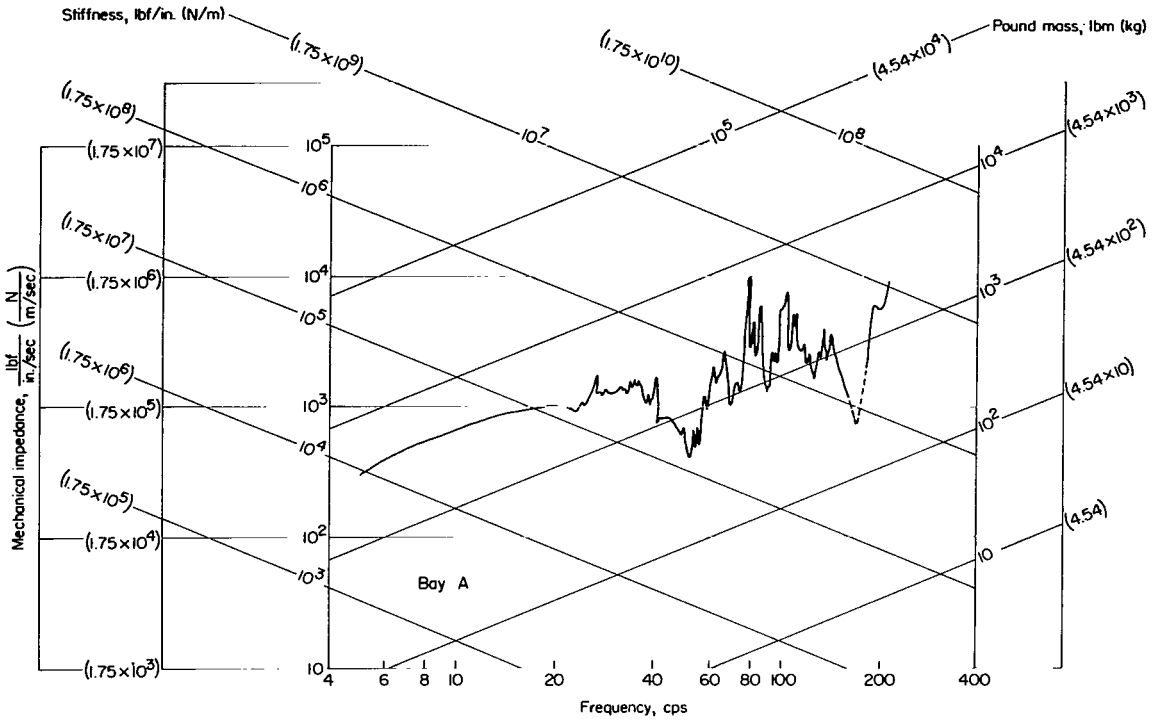

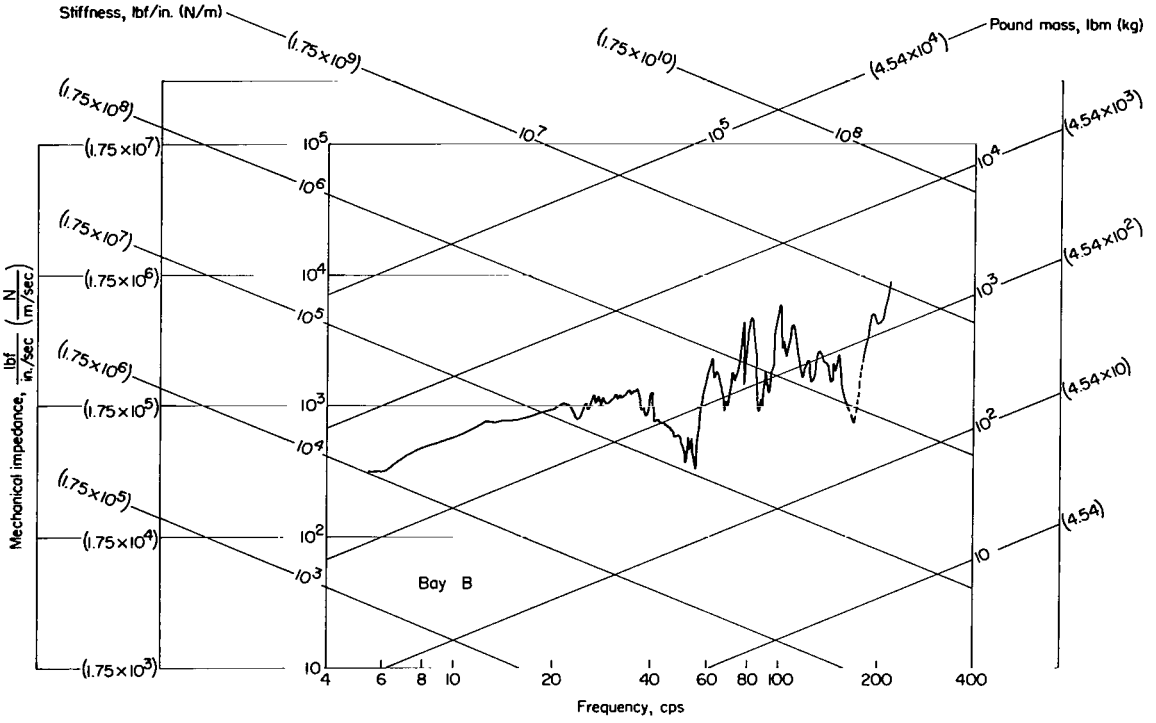

(c) Longitudinal transfer impedance at top of fuel tank in bays A and B. Force input at gimbal point.

Figure 13.- Continued.

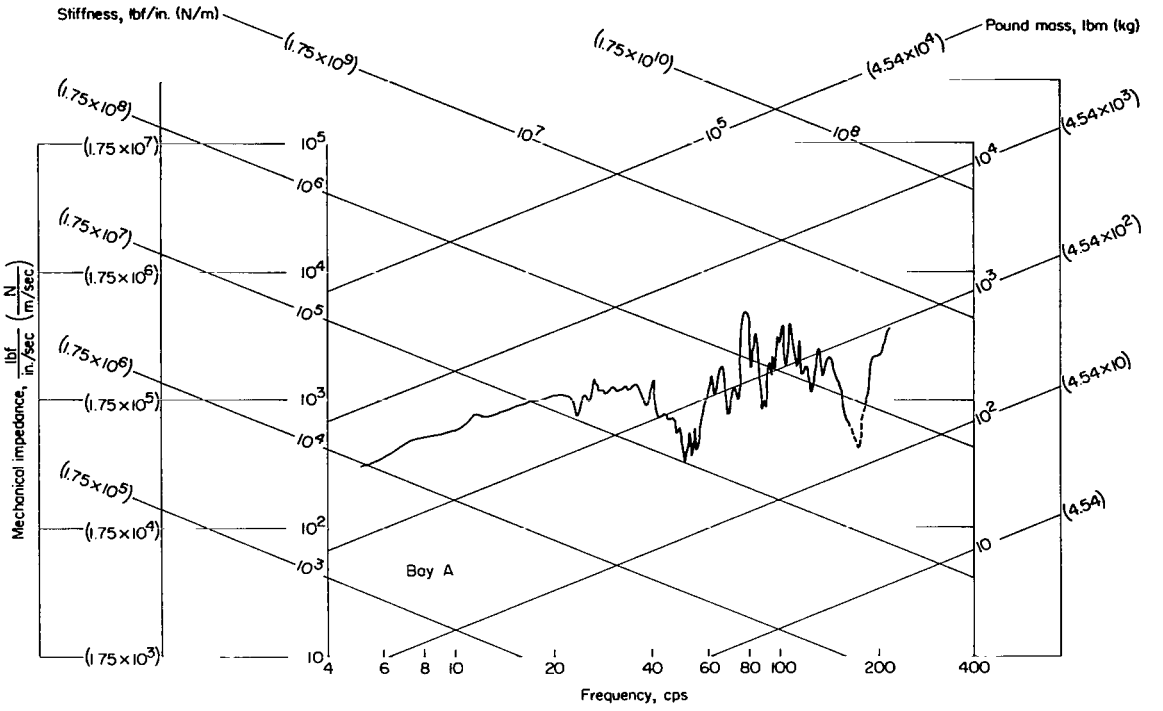

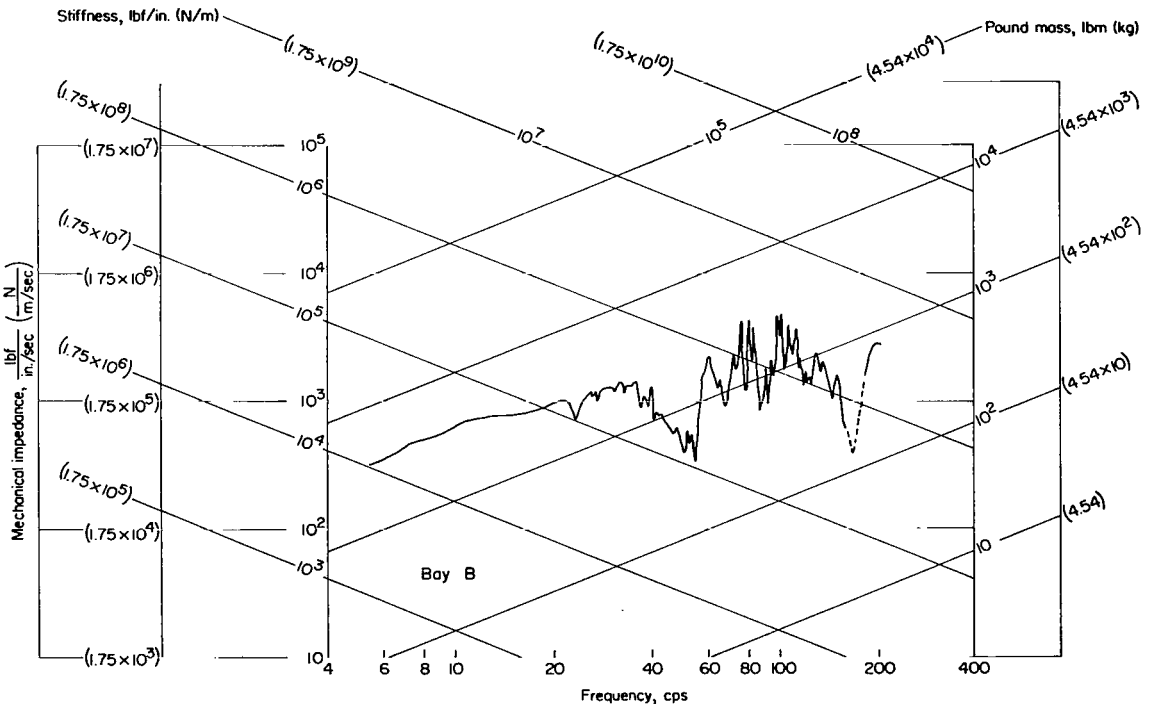

(d) Longitudinal transfer impedance at top of guidance section in bays A and B. Force input at gimbal point.

Figure 13.- Concluded.

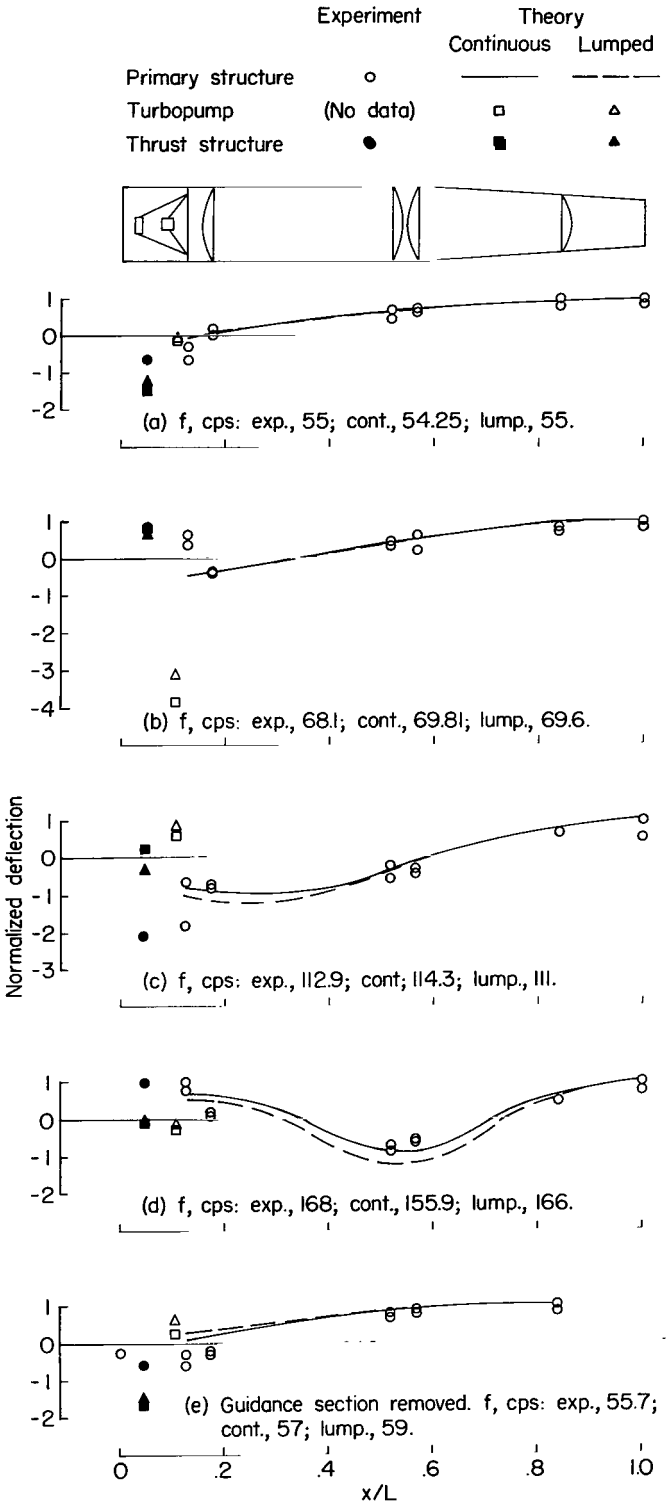

Figure 14.- Comparison of experimental and analytical natural frequencies and mode shapes of the Thor vehicle.

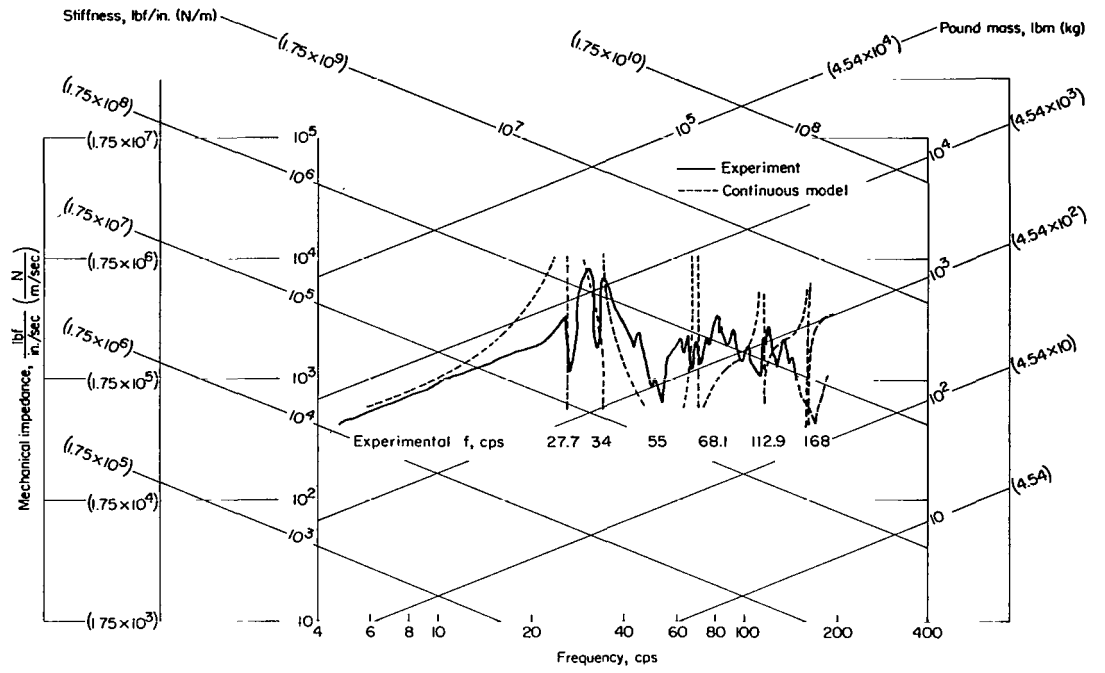

(a) Input impedance at gimbal point. Tanks closed and unpressurized.

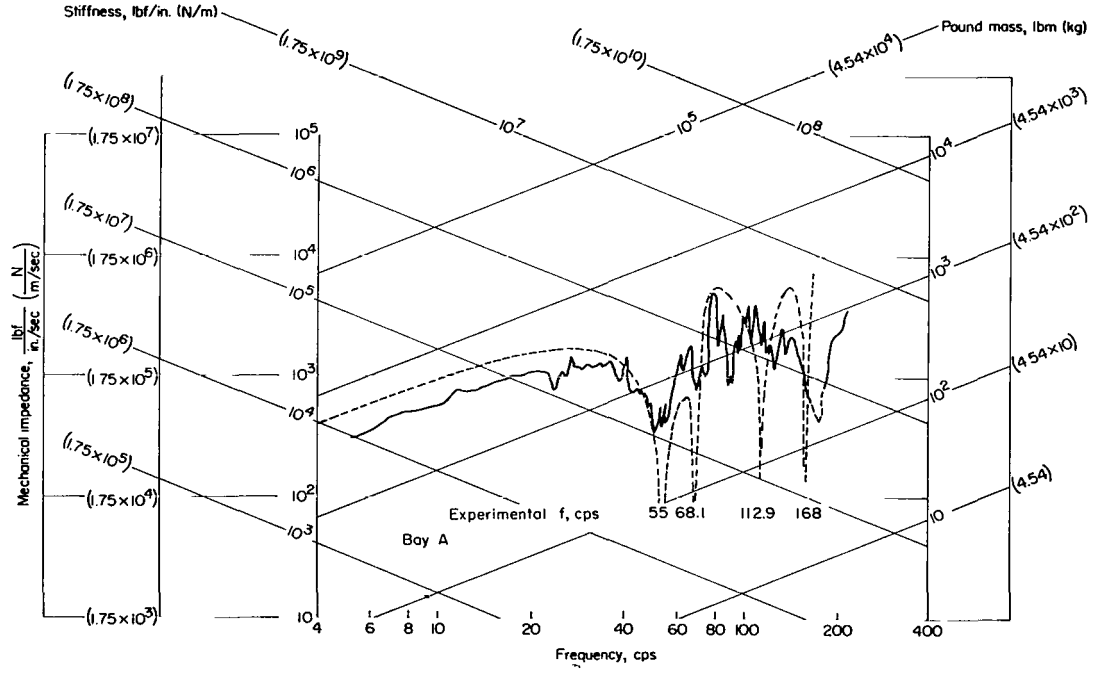

(b) Transfer impedance at top of guidance section. Fuel tank partially vented; LOX tank, closed and unpressurized, containing 50 percent by volume helium-air mixture.

Figure 15.- Comparison of experimental and analytical forced longitudinal response levels of the Thor vehicle.

"The aeronautical and space activities of the United States shall be conducted so as to contribute . . . to the expansion of human knowledge of phenomena in the atmosphere and space. The Administration shall provide for the widest practicable and appropriate dissemination of information concerning its activities and the results thereof."

—NATIONAL AERONAUTICS AND SPACE ACT OF 1958

NASA SCIENTIFIC AND TECHNICAL PUBLICATIONS

TECHNICAL REPORTS: Scientific and technical information considered important, complete, and a lasting contribution to existing knowledge.

TECHNICAL NOTES: Information less broad in scope but nevertheless of importance as a contribution to existing knowledge.

TECHNICAL MEMORANDUMS: Information receiving limited distribution because of preliminary data, security classification, or other reasons.

CONTRACTOR REPORTS: Technical information generated in connection with a NASA contract or grant and released under NASA auspices.

TECHNICAL TRANSLATIONS: Information published in a foreign language considered to merit NASA distribution in English.

TECHNICAL REPRINTS: Information derived from NASA activities and initially published in the form of journal articles.

SPECIAL PUBLICATIONS: Information derived from or of value to NASA activities but not necessarily reporting the results of individual NASA-programmed scientific efforts. Publications include conference proceedings, monographs, data compilations, handbooks, sourcebooks, and special bibliographies.

Details on the availability of these publications may be obtained from:

SCIENTIFIC AND TECHNICAL INFORMATION DIVISION

NATIONAL AERONAUTICS AND SPACE ADMINISTRATION

Washington, D.C. 20546